Molecular Therapy
Nucleic Acids
Original Article

Promotion of tumor progression by exosome transmission of circular RNA circSKA3

William W. Du,[1,5] Xiangmin Li,[1,2,5] Jian Ma,[1] Ling Fang,[1,3] Nan Wu,[1] Feiya Li,[1,4] Preet Dhaliwal,[1] Weining Yang,[1] Albert J. Yee,[1] and Burton B. Yang[1,4]

[1]Sunnybrook Research Institute, Sunnybrook Health Sciences Centre, Toronto, Canada; [2]Guangdong Provincial Key Laboratory of Microbial Safety and Health, State Key Laboratory of Applied Microbiology Southern China, Key Laboratory of Agricultural Microbiomics and Precision Application, Ministry of Agriculture and Rural Affairs, Institute of Microbiology, Guangdong Academy of Sciences; [3]China-Japan Union Hospital of Jilin University, Jilin, China; [4]Department of Laboratory Medicine and Pathobiology, University of Toronto, Toronto, Canada

We performed *in vitro* and *in vivo* experiments to investigate the role of the circular RNA circSKA3 in tumor development. We examined the effects of circSKA3 on mediating breast cancer metastasis. *In vitro*, we found that the circular RNA circSKA3 was transferred between breast cancer cells, which were decreased by inhibiting exosome secretion. *In vivo*, circSKA3-containing exosomes potentiated tumor development and invasion that were inhibited by blocking exosome transmission. The ascites isolated from tumor-bearing mice or breast cancer patients showed high levels of circSKA3 and integrin β1. Single-cell culture and single-cell PCR showed that circSKA3 was heterogeneously expressed, the cells expressing higher levels of circSKA3 had a higher potential to form large colonies. This property was similar to c-myc, but circSKA3 expression had no correlation with c-myc levels. The effects of circSKA3 on cell migration and invasion appeared to predominate c-myc functions. By releasing circSKA3-containing exosomes to cancer cells expressing lower levels of circSKA3, the large colonies could regulate the activities of small colonies, enhancing the tumor-forming capacity of the entire population. Thus, we provide evidence that the transmission of circular RNAs in tumor-derived exosomes may allow for the maintenance of advantageous invasive sub-clones in breast cancer.

INTRODUCTION

Circular RNAs (circRNAs) are a large class of non-coding RNAs that form covalently closed loops. Most circRNAs are generated from exons of pre-mRNAs[1–3] and are abundantly detected in mammalian cells.[4–8] Similar to long non-coding RNAs, some circRNAs have been reported to code for protein peptides.[9–12] Many circRNAs are evolutionarily conserved across species. They thus possess potential regulatory roles.[13] For example, some circRNAs may function as microRNA sponges.[6,14,15] Some circRNAs bind to proteins and regulate their associated signal pathways.[16–18] While binding to proteins, circRNAs form secondary structures and acquire altered conformations.[1,19] This allows circRNAs to modulate gene expression and protein activity through a mechanism distinguishable from their linear mRNA counterparts.[17] Due to these new properties, circRNAs may be involved in the development and progression of many types of cancers.[20–23] This is because circRNAs can regulate various cell activities, including cell proliferation,[20] apoptosis,[24] migration,[25] invasion,[26] and autophagy,[27] as well as wound repair[28] and protein synthesis.[29] In our previous study, we reported that the circRNA circSKA3 was involved in forming invadopodia and cancer invasion.[25] This circRNA is generated by the human gene *SKA3* (spindle- and kinetochore-associated complex subunit 3), which is an essential member of the SKA complex that can stabilize the kinetochore–microtubule interaction during mitosis.[30] SKA3 is involved in tumor cell growth and migration.[31,32] SKA3 can generate many circRNAs: the one used in our study contains 412 nucleotides. Other isoforms have been reported to be involved in exosome formation and medulloblastoma progression.[33,34]

Intra-tumoral heterogeneity underlies the distinct phenotypic profiles of gene expression, epigenetic alterations, and tumor cell metabolism. This heterogeneity remains an underexamined challenge in cancer research and treatment. Currently, two models have been proposed to explain this heterogeneity.[35] The cancer stem cell (CSC) model posits that there are a small number of CSCs[36] that can self-renew and differentiate into non-CSCs and that only CSCs are essential for tumor progression.[37,38] The clonal evolution model proposes that tumors are initiated from individual somatic mutations that sequentially accumulate during tumor progression.[39,40] Increasingly, alterations in non-coding RNAs such as microRNAs and circRNAs have been implicated in the maintenance of tumor heterogeneity and may be integral in the development of resistant or malignant phenotypes. This appears to be mediated by exosomes.[41–43] Exosomes are membrane-bound extracellular vesicles that mediate the transmission of cellular components and signals associated with physiological disorders and cancer development.[44–47] Some cell membrane proteins such as integrins play roles in cancer invasion and metastasis and are present on the exosome surface.[48,49]

Received 20 May 2021; accepted 29 November 2021;
https://doi.org/10.1016/j.omtn.2021.11.027.

[5]These authors contributed equally

Correspondence: Burton B. Yang, Sunnybrook Research Institute, Sunnybrook Health Sciences Centre, S-Wing Research Building, 2075 Bayview Avenue, Toronto M4N 3M5, Canada.
E-mail: byang@sri.utoronto.ca

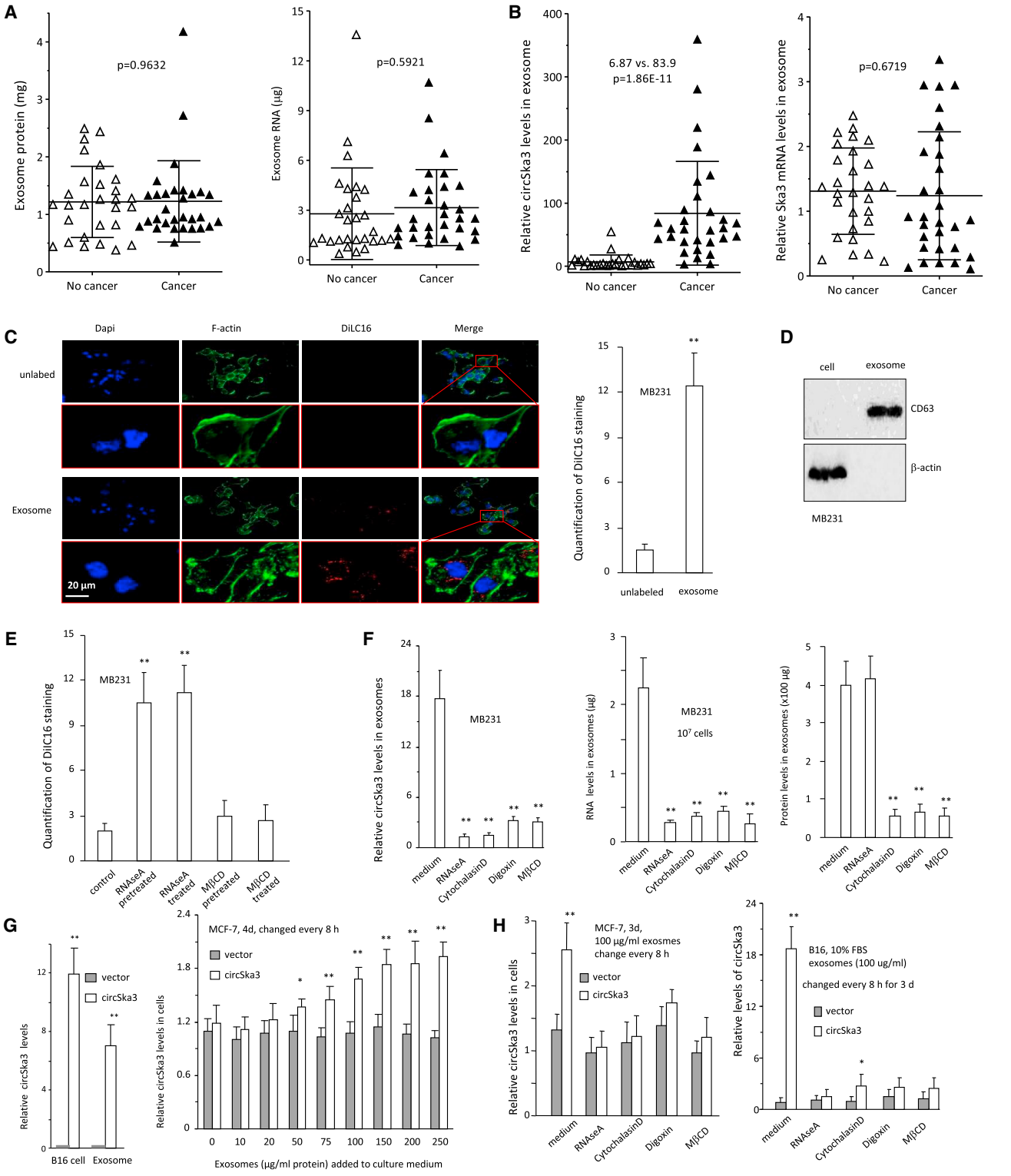

Figure 1. Exosome-mediated transfer of circSKA3

(A) Ascites exosomes isolated from 29 cancer patients and 30 non-cancer patients (10 mL ascites from each) were quantified to measure levels of total protein (left) and RNAs (right). No significant difference was detected in the two groups of samples. (B) Exosomes isolated from ascites of 29 cancer patients and 30 non-cancer patients (10 mL

(legend continued on next page)

RESULTS

Exosomal transmission of circSKA3 promotes cell invasion

Our previous paper showed that the circRNA circSKA3 formed invadopodia with integrin β-1 and promoted cancer cell invasion.[25] We hypothesized that circSKA3 was included in the exosomes and transmitted between cancer cells. To test this hypothesis, we isolated exosomal fractions from ascites fluids of breast cancer patients and measured circSKA3 expression in the exosomes. We measured the total protein and mRNA levels in the exosomes isolated and confirmed similar levels in all samples (Figure 1A). We then measured the levels of circSKA3 using divergent primers specific for circSka3 and levels of SKA3 linear mRNA using primers outside circSKA3. While there were no significant differences in the levels of SKA3 mRNA, we found that cancer patients expressed significantly higher levels of circSKA3 relative to healthy individuals (Figure 1B).

We also isolated exosomes from the medium of DiIC16-labeled cells and applied them to MDA-MB-231 cultures. Exosomes entering MDA-MB-231 cells were detected by DiIC16 staining (Figure 1C). We used the exosome marker CD63 to confirm the successful isolation of exosomes (Figure 1D). To validate the entering of exosomes, we pretreated cells with or without RNAse A or methyl-β-cyclodextrin (MβCD). The medium was added to MDA-MB-231 cell cultures and was followed by treatment with RNAse A or MβCD. Exosomes entering MDA-MB-231 cells were measured by DiIC16 staining. Treatment with MβCD inhibited exosomes entering the cells, but treatment with RNAse A did not (Figure 1E; photos provided in Figure S1).

We have recently found that the circRNA circSKA3 plays a role in enhancing tumor cell invasion. We examined whether this effect was mediated by exosome transmission. Exosomes were harvested from MDA-MB-231 cells treated with reagents, including RNAse A, Cytochalasin D, Digoxin, and MβCD, which are involved in exosome transmission. These chemicals disrupt exosomal transmission by inhibiting lipid raft formation (MβCD), actin polymerization (Cytochalasin D) and ATPase (Digoxin). All chemicals repressed the circSKA3 expression levels in exosomes (Figure 1F). RNAse A treatment decreased total RNA levels including circSKA3 but had no effect on the total exosome amount in the cultured cell medium, whereas Cytochalasin D, Digoxin, and MβCD repressed the total amount of exosomes in the cell medium, indicating that these inhibitors could suppress exosome secretion into the cell medium.

We also tested the transmission of circSKA3-containing exosomes in different cell types. Exosomes were isolated from circSKA3- and vector-transfected B16 cells and added to MCF-7 cell cultures. Cells and exosomes from the circSKA3-transfected cells had increased levels of circSKA3 relative to the controls (Figure 1G, left). The increased uptake of circSKA3 by MCF-7 cells was concentration-dependent (Figure 1G, right). The increased uptake of circSKA3 by MCF-7 and B16 cells was abolished upon treatments with RNAse A, Cytochalasin D, Digoxin, and MβCD (Figure 1H).

We evaluated the heterogenicity of circSKA3 in cancer cells. MDA-MB-231 cells were treated with RNAse A, Cytochalasin D, Cyclodextrin (MβCD), and Digoxin, followed by a single-cell PCR measurement of circSKA3 levels. Most of the cells, after being treated with these reagents, displayed decreased circSKA3 in the single-cell culture (Figure 2A). Treatment with these reagents (excluding RNAse A) that play roles in exosome transmission, however, significantly increased the levels of circSKA3 in a small proportion of cells (Figure 2A). These results showed that there were only a small proportion of cells that expressed extremely high levels (50- to 100-fold) of circSKA3 relative to the majority of the cell population. To test the effect of exosome-packaged circSKA3, we added the exosome-containing medium into MCF-7 cell cultures and found that this significantly promoted cell invasion (Figures 2B and S2A). Decreasing the exosome uptake by treatment with RNAse A, Cytochalasin D, Digoxin, and MβCD abolished the enhanced cell invasion (Figures 2C and S2B). In a wound-healing assay, MCF-7 cells were cultured in basal medium, in which 100 μg/mL exosomes harvested from vector- or circSKA3-transfected cells were added. circSKA3-packed exosomes enhanced cell migration (Figures 2D and S3A). In chamber migration assays, circSKA3-packed exosomes also enhanced cell locomotion to the bottom surface of the wells (Figures 2E and S3B). The addition of RNAse A or the reagents (Cytochalasin D, Digoxin, and MβCD) abolished the effect of circSKA3 on cell migration in the wound-healing and chamber migration assays (Figures 2F and S4).

Exosomal transmission of circSKA3 promotes cancer progression

We then tested the effect of circSKA3 on tumor development *in vivo*. Nude mice bearing MDA-MB-231 tumor xenografts in the abdomen were intraperitoneally injected with control oligonucleotide (oligo), circSKA3 siRNA, RNAse A, MβCD, or Digoxin. We found that

ascites from each) were quantified to measure the levels of circSKA3 (left) and SKA3 linear mRNA (right). Significantly higher levels of circSKA3 were detected in cancer patients relative to non-cancer patients. (C) Left, exosomes were isolated from the medium of DiIC16-labeled MB-231 cells (exosome) or the DiIC16-containing medium (control) and applied to MB-231 cell cultures. After 24 h incubation, the cells were stained with DAPI (blue) for nucleus, green fluorescence showing F-actin, and red fluorescence showing DiIC16 (exosome). Right, quantification of exosomes entering MB-231 cells. (n = 6). (D) Western blot showing the presence of exosome marker CD63 in the preparation. (E) Exosomes isolated from the medium of DiIC16-labeled cells were applied to MB-231 cultures for 24 h before detection for fluorescent DiIC16. The RNAse A or methyl-β-cyclodextrin (MβCD) pre-treated samples were treated with RNAse A or MβCD during DiIC16 staining, while the RNAse A or MβCD-treated cells were cultured with a conditioned medium with RNAse A or MβCD for 24 h. Exosomes entering MB-231 cells could be prevented by MβCD but not RNAse A. (F) Total exosomes were isolated from a culture medium of MB-231 cells treated with 1 μM Cytochalasin D, 0.4 μM Digoxin, 1 mM MβCD, or 1 μg/mL RNAse A, followed by the measuring of the levels of circSKA3 (left), RNA (middle), and proteins (right). All inhibitors repressed these components entering exosomes (n = 4). (G) Left, circSKA3-transfected B16 cells and exosomes isolated from the cells contained significantly higher levels of circSKA3 relative to controls. Right, the addition of exosomes isolated from the circSKA3-transfected B16 cells increased the uptake of circSKA3 in MCF-7 cells (n = 3). (H) Total exosomes were isolated from a culture medium of control vector- and circSKA3-transfected B16 cells. The increased levels of circSKA3 in the circSKA3-containing exosomes entering MCF-7 (left) and B16 (right) cells were prevented by RNAse A, Cytochalasin D, Digoxin, and MβCD (n = 4), * $p<0.05$; ** $p<0.01$; Error bars, SD.

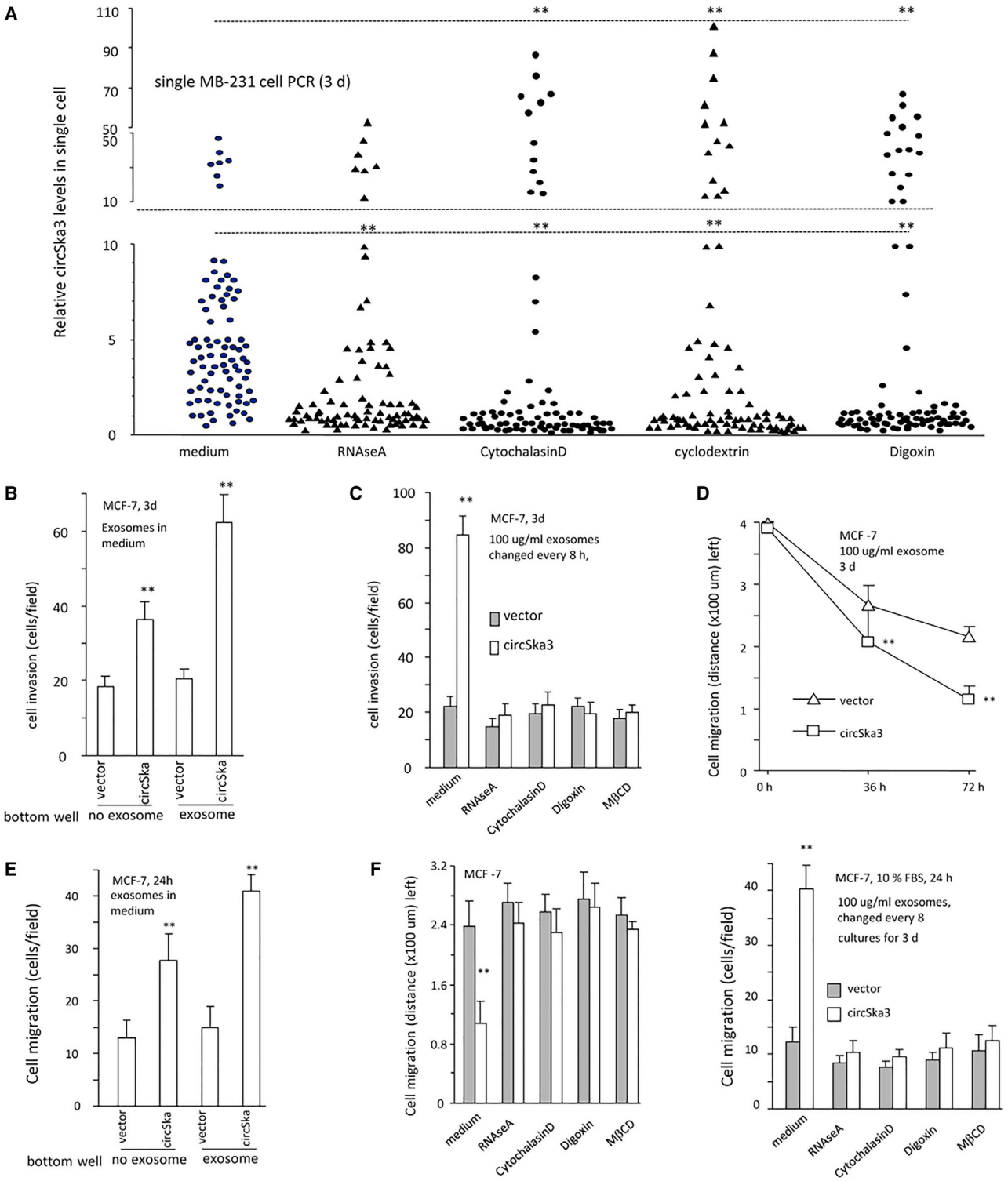

Figure 2. Inhibition of exosome secretion decreased circSKA3 transfer

(A) Single-cell PCR showed that approximately 5%–10% cells (HIGH) expressed significantly higher levels of circSKA3 than other cells (LOW). Treatment with Cytochalasin D, Digoxin, or MβCD did not affect the average levels of circSKA3 in the cells but decreased cricSKA3 levels in the LOW cells and increased circSKA3 levels in the HIGH cells. Treatment with RNAse A only decreased cricSKA3 levels in the LOW cells relative to the medium control. (n = 80). (B) circSKA3-packed exosomes enhanced MCF-7 cell

(legend continued on next page)

silencing endogenous circSKA3 or inhibiting the exosome transmission decreased tumor development and extended the life span of mice significantly (Figure 3A). Tumor tissues were subjected to real-time PCR to measure circSKA3 levels. As expected, treatment with circSKA3 siRNA decreased circSKA3 levels in the tumors (Figure 3B). Treatment with RNAse A, MβCD, or Digoxin also decreased circSKA3 levels but not as much as small interfering RNA (siRNA) treatment. The tumors were also sectioned for *in situ* hybridization. Quantitation of circSKA3 confirmed the decreased levels of circSKA3 in the tumors treated with circSKA3 siRNA, RNAse A, MβCD, or Digoxin (Figure 3C). An analysis of exosomal fractions from ascites of these mice and from intra-tumoral circRNA showed decreased levels of circSKA3 in mice treated with circSKA3 siRNA, RNAse A, MβCD, or Digoxin (Figure 3D). Total RNA levels in the exosomes decreased in mice injected with RNAse A, Digoxin, or MβCD, while total protein levels were lower in mice injected with Digoxin or MβCD (Figure 3D). This confirmed that circSKA3 siRNA and RNAse A did not affect the amount of exosomes in the ascites. These results were corroborated by single-cell PCR using cells isolated from the tumors. Treatment with Digoxin or MβCD did not affect the average levels of circSKA3 in the tumor cells but decreased the circSKA3 levels in the LOW (bottom 10%) cells and increased the circSKA3 levels in the HIGH (top 10%) levels (Figure 3E). Treatment with RNAse A only decreased the circSKA3 levels in the LOW cells. These extreme levels of circSKA3 suggest an inhibitory effect of tumor-tumor exosomal transmission of circSKA3.

We also injected normal C57 mice with B16 tumor cells to test exosomal transmission. After injection with B16 cells, C57 mice were intraperitoneally injected with B16 culture medium-derived exosomes with or without exosome transmission inhibitor treatment. Injection with circSKA3-containing exosomes promoted tumor progression and decreased mouse viability, which was reversed by the delivery of the exosome transmission inhibitors (Figure 4A). Analysis of ascites showed an accumulation of circSKA3 in the mouse exosomes treated with MβCD and Digoxin, while decreased levels of total RNA and protein levels in exosomes indicated that MβCD and Digoxin blocked exosome secretion (Figure 4B). Treatment with these reagents also decreased the circSKA3 levels in the tumor tissues (Figure 4C). The ascites, tumor cells, and tumor xenografts were obtained from circSKA3-transfected B16 cells and MDA-MB-231 cells. The ascites contained the highest level of circSKA3, followed by the tumors, while SKA3 mRNA was mainly detected in the tumor tissues (Figure 4D).

The ascites fluid was incubated with B16 cells, followed by confocal examination. This provided direct evidence that circSKA3-containing exosomes were uptaken by the cells. The ascites from tumor-bearing mice injected with circSKA3-transfected B16 cells or from MDA-MB-231 cell cultures displayed increased levels of circSKA3 (Figure 5A). In a cell invasion assay, ascites from mice injected with circSKA3-transfected B16 cells or from MB-231 cell cultures enhanced cell invasion (Figure 5B) and migration (Figure 5C). Treatment with exosome transmission inhibitors abolished uptake of circSKA3 (Figure 5D), subsequently impeding cell migration and invasion (Figure 5E). We also analyzed tumor sections formed by MDA-MB-231 cells and found that treatment with MβCD or with circSKA3 siRNA decreased tumor invasion *in vivo* (Figure 5F).

Integrin β1 and Tks5 are exosomally transmitted with circSKA3

We have recently shown that circSKA3 formed invadopodia by binding to integrin β1 and TKS5. It has been reported that integrins are important components in exosome formation.[50] We examined whether circSKA3 binding to integrin β1 and TKS5 formed invadopodia that were involved in exosome formation. On the other hand, the transmitted exosomes could also promote the formation of invadopodia in the recipient cells. To test these possibilities, we measured invadopodia levels in the nude mice injected with MDA-MB-231 cells, followed by the delivery of inhibitors for exosome transmission. Tumors from mice injected with circSKA3 siRNA, RNAse A, MβCD, or Digoxin formed lower amounts of invadopodia (Figures 6A and S5A), suggesting that circSKA3-containing invadopodia are involved in exosome formation, and the transmission of exosomes increased invadopodia levels in the tumors. In normal mice injected with B16 cells, injection with circSKA3-containing exosomes enhanced invadopodia formation, while injection with inhibitors for exosome transmission (RNAse A, MβCD, or Digoxin) abolished the effect of circSKA3-containing exosomes on invadopodia formation (Figures 6B and S5B). B16 cells cultured with ascites fluid harvested from mice bearing circSKA3-expressing xenografts formed more invadopodia (Figure S6). This finding was abolished by exosome inhibitor treatment (Figure S7).

The ascites harvested from mice bearing circSKA3-expressing xenografts promoted invadopodia formation in the recipient cells. MCF-7 cells cultured with or without ascites displayed higher levels of integrin β1 and Tks5 in the total invadopodia fraction (Figure 6C). B16 cells cultured with ascites increased levels of circSKA3 (Figure S8A) and invadopodia in a gelatin assay (Figure S8B). When the preparation of circSKA3-containing exosomes was cultured with B16 cells, circSKA3 was enriched in the invadopodia of the cells, which also increased Tks5 and integrin β1 levels in the invadopodia-

invasion (n = 4). (C) The invasion of MCF-7 cells was inhibited by RNAse A, Cytochalasin D, Digoxin, and MβCD (n = 4). (D) MCF-7 cells were cultured in a basal medium with 100 μg/mL control vector- or circSKA3-packed exosomes and processed to wound-healing assays for 3 days, showing that circSKA3-packed exosomes enhanced cell migration (n = 6). (E) MCF-7 cells were cultured in a basal medium with 100 μg/mL control vector- or circSKA3-packed exosomes for 3 days and processed to chamber migration assays with 100 μg/mL control vector- or circSKA3-packed exosomes at the bottom wells for 3 days. circSKA3-packed exosomes enhanced MCF-7 cell migration (n = 4). (F) Left, MCF-7 cells were cultured in a basal medium with 100 μg/mL control vector- or circSKA3-packed exosomes and chemicals RNAse A, Cytochalasin D, Digoxin, or MβCD for 3 days and processed to wound-healing assays. circSKA3-packed exosomes enhanced cell migration, which could be prevented by RNAse, Cytochalasin D, Digoxin, and MβCD. Right, in chamber migration assays, circSKA3-packed exosomes enhanced cell migration, which could be prevented by RNAse A, Cytochalasin D, Digoxin, and MβCD (n = 4), * $p<0.05$; ** $p<0.01$; Error bars, SD.

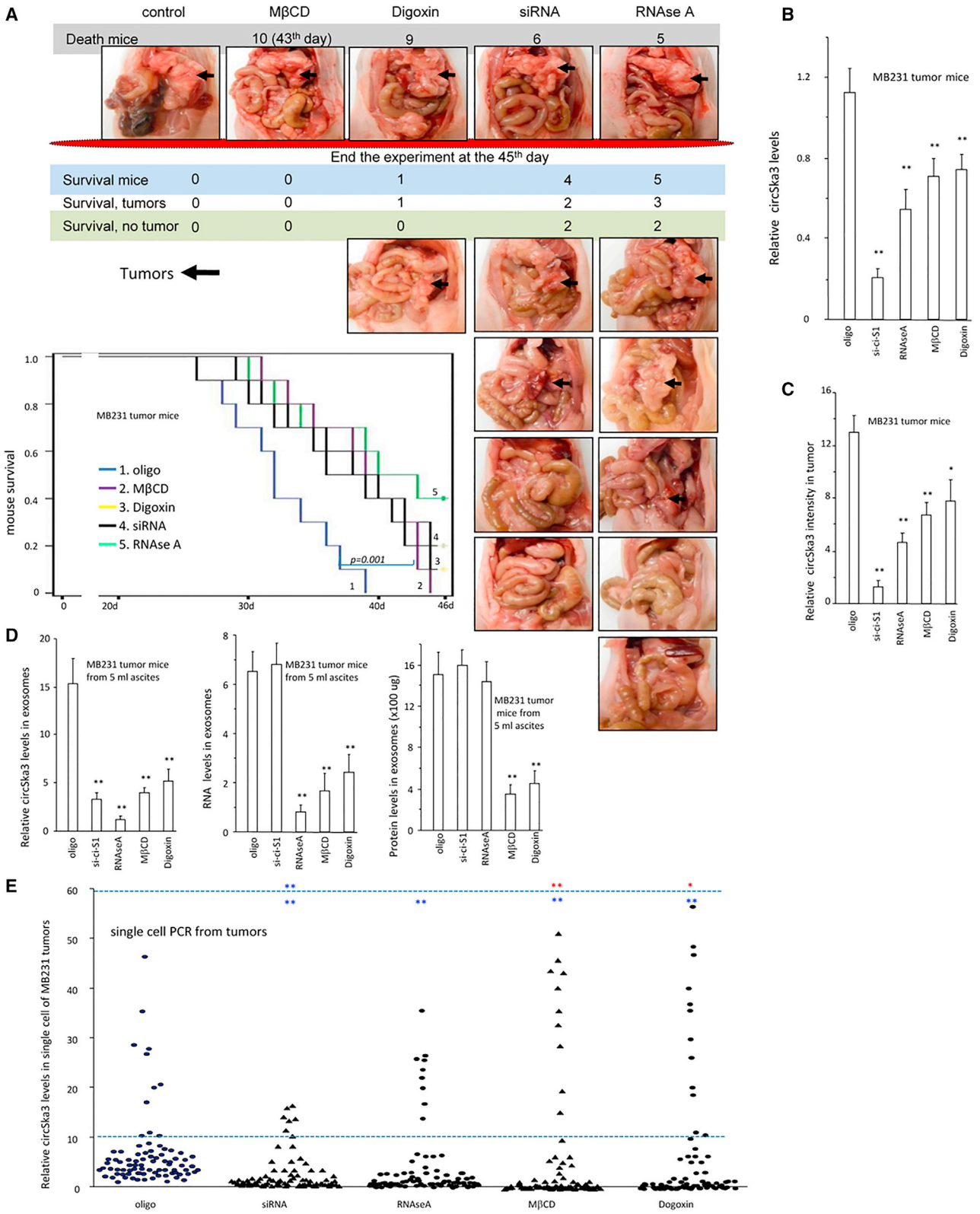

(legend on next page)

containing membrane (Figure 6D). This suggests that Tks5 and integrin β1 are exosomally co-transmitted with circSKA3.

MCF-7 cells transfected with circSKA3 produced increased levels of circSKA3, Tks5, and integrin β1 (Figure 6E). B16 cells transfected with circSKA3 formed more invadopodia in the gelatin assay, which was inhibited by inhibitors of exosome transmission (Figure S9). Exosomal circSKA3 could be precipitated by antibodies against Tks5 and integrin β1 (Figure 6F). Increased levels of these proteins were detected in exosomes from cells overexpressing circSKA3. Conversely, a circSKA3 probe could precipitate higher levels of Tks5 and integrin β1 from exosomes harvested from cells transfected with circSKA3 (Figure 6G). As expected, silencing circSKA3 or integrin β1 decreased invadopodia formation in the gelatin assay (Figure S10).

Exosomal transfer of circSKA3 confers an invasive phenotype to recipient tumor cells

Given the heterogeneous expression levels of circSKA3, we next examined whether circSKA3 could be transmitted from tumor cells expressing high levels of circSKA3 to those expressing lower levels. We randomly cultured individual cells in 96-well plates to obtain one cell per well. A total of 3,662 colonies (wells) were obtained, which showed a diverse number of cells in each colony (Figure 7A). Measurements of circSKA3 levels revealed higher levels of circSKA3 in the large colonies than the small colonies and the low-invasion colony (LIC) (Figure 7B). Since c-myc is a well-known oncogene, we measured its levels to estimate the correlation between the circSKA3 and c-myc levels. We found that the levels of c-myc were also higher in the large colonies (Figure 7C). We analyzed the levels of circSKA3 and c-myc in the 167 large colonies and found that there was no correlation between circSKA3 and c-myc (Figure 7D). We grouped these colonies into HIGH (top 10%) and LOW (bottom 10%) levels of circSKA3 and c-myc measured by real-time PCR. The colonies were subjected to cell invasion (Figure 7E) and migration (Figure 7F) assays. It appeared that the large colonies with high levels of circSKA3, but not c-myc, were essential for the promotion of cell migration and invasion. This indicated that the role of circSKA3 in cell migration and invasion overrode that of c-myc. This was supported by increased vimentin and N-cadherin but decreased E-cadherin levels (Figures S11A–S11C), essential molecules in regulating cell migration and invasion. Nevertheless, the levels of Sox2 and Oct4 appeared to be regulated by c-myc (Figures S11D and S11E).

We isolated large colonies that expressed high levels of circSKA3 and cultured them in 96-well plates. The cells were subjected to single-cell PCR. These large-colony cells could not maintain high levels of circSKA3 after a re-culture. Instead, they acquired a pattern similar to regular cells (Figure 7G), allowing a few cells to maintain high levels of circSKA3. This suggests that heterogeneity occurred immediately when the cells were re-cultured, retaining a small population of cells expressing high levels of circSKA3. In other words, there is always a small number of cells that can express high levels of circSKA3 in a cell population.

We wondered whether circSKA3 could be transmitted from tumor cells expressing high levels of circSKA3 to those expressing lower levels of circSKA3. We found significantly increased circSKA3 levels in cells cultured in the medium harvested from circSKA3-transfected cells (Figure 8A). Cells that expressed high levels of circSKA3 displayed high invasion abilities (Figure 8B). The addition of exosomes isolated from circSKA3-transfected cells increased the levels of circSKA3 in the cells (Figure 8C), suggesting an uptake of circSKA3-containing exosomes. Furthermore, we observed that a co-culture with cells expressing high levels of circSKA3 conferred a large quantity of circSKA3 to tumor cells with low invasive potential (Figure 8D), resulting in increased cell migration in those cells (Figure 8E). We verified these results by single-cell PCR following a co-culture. LICs were co-cultured with small-colony cells, large-colony cells (circSKA3^{H}/c-myc^{H}), and LICs co-cultured with the large-colony cells and MβCD. A co-culture with large-colony cells increased the levels of circSKA3 and resulted in a similar pattern as the regular cells, which could be blocked by MβCD (Figure 8F). This indicated a transmission of circSKA3-containing exosomes from the large-colony cells to the LIC cells, which were blocked by the exosome transmission inhibitor MβCD.

DISCUSSION

It has been recently reported that circRNAs can be secreted from tumor cells by exosomes.[51] We show here that circRNA-containing exosomes can then be taken up by neighboring tumor cells. Another class of non-coding RNAs, microRNAs, have been demonstrated to be transmitted between cells, thereby regulating tumorigenesis.[52–54] Since microRNAs regulate gene expression by targeting the 3′ UTR of messenger RNAs, it is conceivable that microRNAs must be transmitted through exosomes at a sufficient copy number to reach the threshold of regulation as sponges. circRNAs exert biological

Figure 3. circSKA3-containing exosomes potentiate tumor invasion

(A) After injection with MB-231 cells, CD-1 nude mice were also injected with control oligo, circSKA3 siRNA, RNAse A, MβCD, or Digoxin. The delivery of circSKA3 siRNA, RNAse A, MβCD, or Digoxin increased mouse viability significantly, relative to controls (log rank test, **$p < 0.01$). (B) PCR showed that the circSKA3 levels in the tumor tissues decreased when mice were injected with circSKA3 siRNA, RNAse A, Digoxin, or MβCD (n = 6). (C) ImageJ showed that the circSKA3 levels in the tumor tissues decreased when mice were injected with circSKA3 siRNA, RNAse A, Digoxin, or MβCD (n = 6). (D) circSKA3 levels in the exosomes decreased when mice were injected with circSKA3 siRNA, RNAse A, Digoxin, or MβCD (left). Total RNA levels in the exosomes of tumor tissues decreased when mice were injected with RNAse A, Digoxin, or MβCD (middle). Total exosomes of mouse ascites were lower when mice were injected with Digoxin or MβCD (right) (n = 5). (E) Single-cell PCR showed that approximately 8%–10% of cells (HIGH) expressed significantly higher levels of circSKA3 than other cells (LOW). Treatment with RNAse A, Digoxin, or MβCD did not affect the average levels of circSKA3 in the cells but decreased the circSKA3 levels in the LOW cells and increased the circSKA3 levels in the HIGH levels. Treatment with RNAse A only decreased circSKA3 levels in the LOW cells. Upper of the dotted line, HIGH expression; lower of the dotted line, LOW expression; red, upregulated; blue, downregulated. (n = 80), * $p<0.05$; ** $p<0.01$; Error bars, SD.

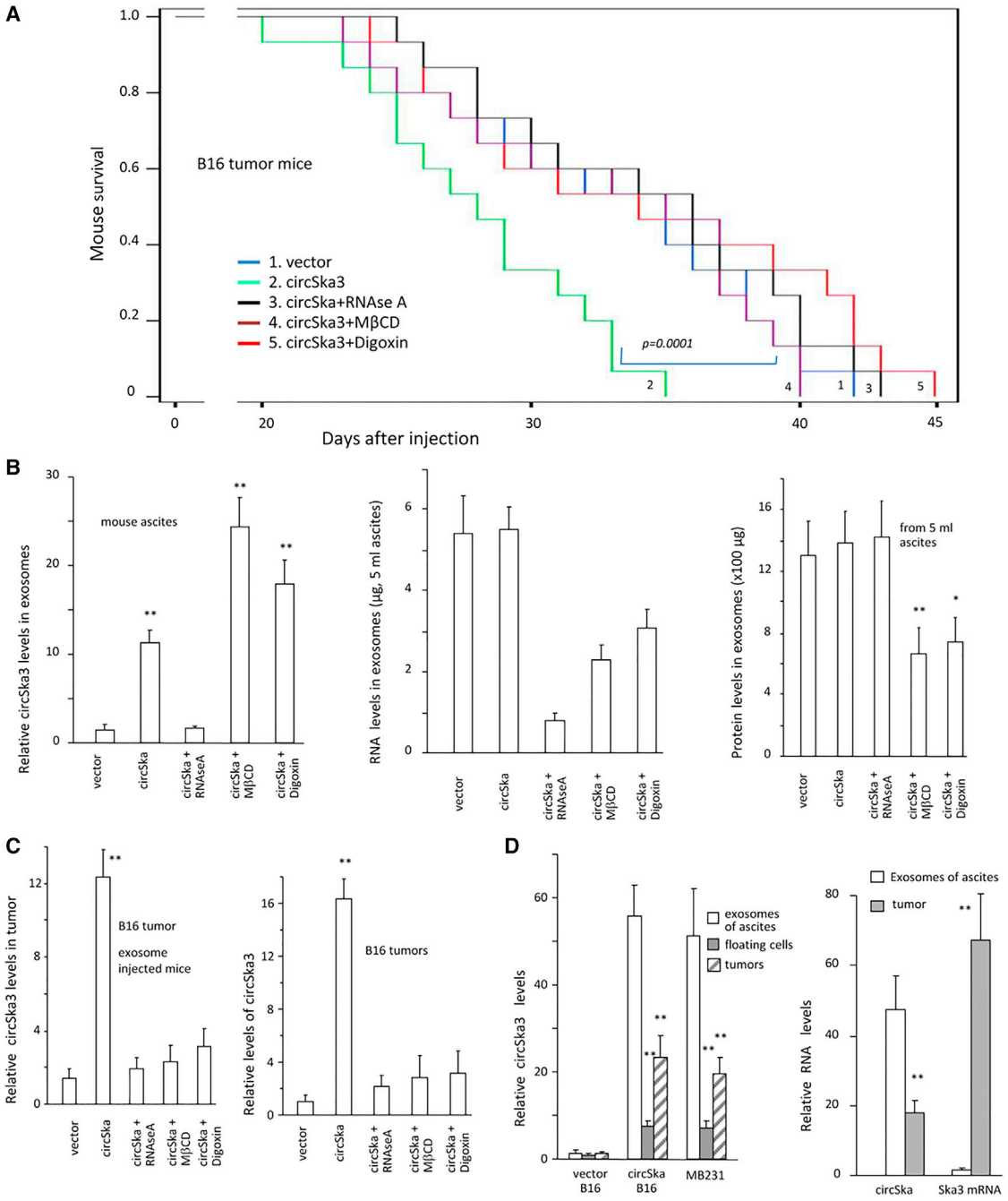

Figure 4. Blocking exosome transmission decreased tumor development

(A) After injection with B16 cells, C57 mice were intraperitoneally injected with exosomes. Injection with circSKA3 exosomes decreased mouse survival significantly, which could be prevented by the delivery of RNAse A, Digoxin, or MβCD (n = 10). (B) circSKA3 levels decreased when mice were injected with RNAse A (left). Total RNA levels in the exosomes decreased when mice were injected with RNAse A, Digoxin, or MβCD (middle). Total exosome levels decreased when mice were injected with Digoxin or MβCD (right) (n = 6). (C) Left, real-time PCR measurement of the tumor tissues showed that injection with circSKA3-containing exosomes increased the circSKA3 levels in tumor tissues, which could be blocked by injection with RNAse A, Digoxin, or MβCD. Right, *in situ* hybridization staining was performed in tumor sections followed by quantitation. Injection with circSKA3-containing exosomes increased circSKA3 uptake in the tumors, which was prevented by the application of RNAse A, Digoxin, or MβCD (n = 6). (D) Ascites, floating cells, and tumors from mice injected with circSKA3-transfected B16 cells or MB-231 cells were analyzed for circSKA3 levels. circSKA3 was detected at the highest level in ascites (left), while SKA3 mRNA was mainly detected in the tumors (right) (n = 6), * $p<0.05$; ** $p<0.01$; Error bars, SD.

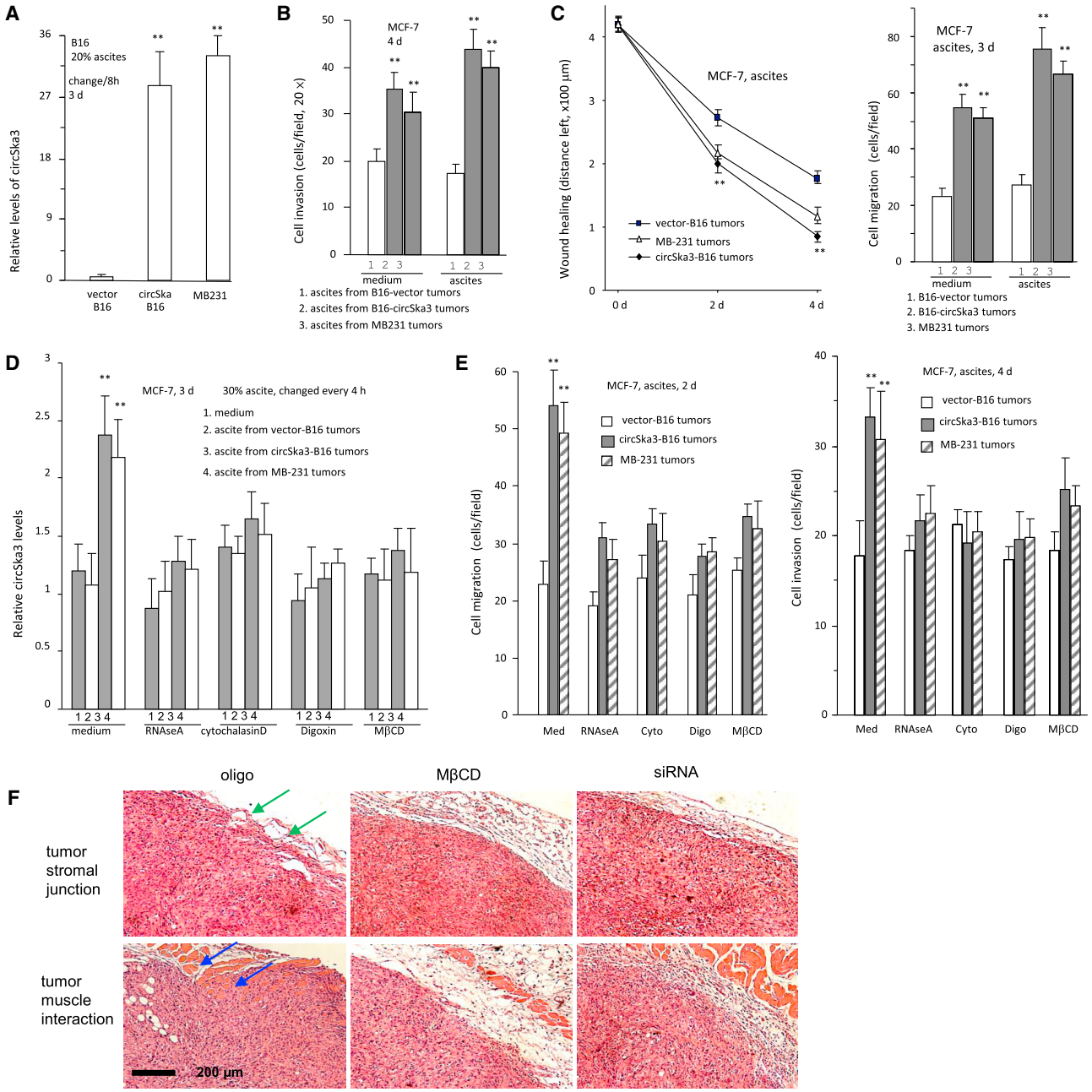

Figure 5. Tumor ascites is the major source of exosome and circSKA3

(A) B16 cells were incubated with a basal medium with 20% mouse ascites for 3 days followed by immunostaining and ImageJ analysis. Ascites from tumor-bearing mice injected with circSKA3-transfected B16 cells or MB-231 cells displayed increased levels of circSKA3 (n = 6). (B) MCF-7 cells were cultured in a basal medium with 20% ascites from mice injected with cells for 3 days and subjected to an invasion assay with or without ascites at the lower wells. Ascites from mice injected with circSKA3-transfected B16 or MB-231 cells enhanced cell invasion (n = 4). (C) MCF-7 cells were cultured with 30% ascites from mice injected with B16 or MB-231 cells. Treatment with ascites from tumor-bearing mice injected by circSKA3-transfected B16 or MB-231 cells increased cell motility in wound-healing (left) and chamber migration (right) assays (n = 4). (D) MCF-7 cells were cultured with 30% ascites from mice injected with B16 or MB-231 cells. Treatment with ascites of tumor-bearing mice injected by circSKA3-transfected B16 or MB-231 cells increased the circSKA3 uptake into MCF-7 cells, which was prevented by RNAse A, Cytochalasin D, Digoxin, and MβCD (n = 3). (E) Ascites from mice injected with circSKA3-transfected B16 or MB-231 cells enhanced MCF-7 cell migration in Transwell (left) and cell invasion in Matrigel (right), which could be blocked by RNAse A, Cytochalasin D, Digoxin, and MβCD treatment (n = 3). (F) Tumor sections were subjected to H&E staining. Tumors formed by MB-231 cells showed invasion into the connective stroma (green arrows) and muscles (blue arrows) in the oligo-treated samples that were blocked by treatment with MβCD and circSKA3 siRNA, * $p<0.05$; ** $p<0.01$; Error bars, SD.

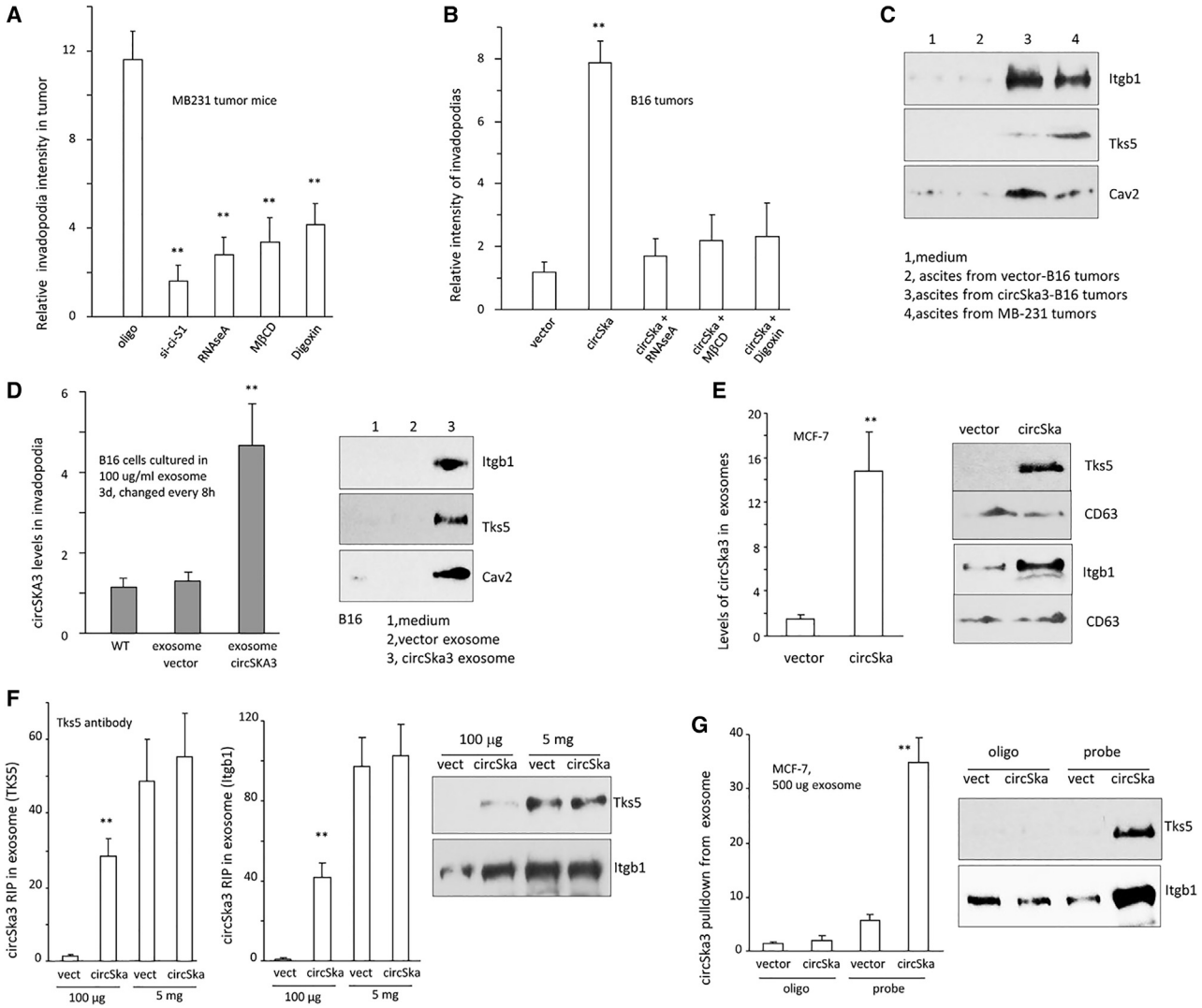

Figure 6. Integrin β1 is exosomally transmitted with circSKA3

(A) Invadopodia formation was repressed in the tumor tissues when mice were injected with circSKA3 siRNA, RNAse A, MβCD, or Digoxin (n = 6). (B) Injection with circSKA3-containing exosomes promoted invadopodia formation, which was blocked by RNAse A, Digoxin, or MβCD (n = 6). (C) MCF-7 cells were cultured with 20% ascites from mice injected with tumor cells. Integrin β1, Tks5, and Cav2 proteins were detected in the invadopodia cultured with ascites of mice injected with circSKA3-transfected B16 cells or MB-231 cells. (D) Left, B16 cells were loaded on gelatin-coated culture dishes and cultured in a basal medium with 100 μg/mL control vector- or circSKA3-packed exosomes for 3 days, followed by invadopodia collection and RNA extraction. Ascites from tumor-bearing mice injected with circSKA3-transfected B16 cells increased circSKA3 levels in invadopodia of the cultured B16 cells. (n = 4). Right, integrin β1, Tks5, and Cav2 proteins were detected in the exosomes harvested from B16 cells transfected with or without circSKA3. CD63 was enriched in the isolated exosomes from a MB-231 culture medium. (E) Exosomes isolated from cells transfected with circSKA3 expressed higher levels of Tks5 and integrin β1. (F) RIP showed that circSKA3 was precipitated from exosomes by antibodies against Tks5 (left) and integrin β1 (middle). Increased levels of these proteins were detected in the exosomes (100 μg or 5 mg protein) from cells overexpressing circSKA3 (right). (G) The circSKA3 probe pulled down higher levels of Tks5 and integrin β1 from exosomes harvested from cells transfected with circSKA3, ** $p<0.01$; Error bars, SD.

functions through at least two mechanisms: microRNA sponging or protein binding. To function as microRNA sponges, there must be a sufficiently high number of either microRNA binding sites or circRNA copy numbers. However, to modulate cell function by protein binding, it is plausible that these are not the requirements. Given the stability of circRNAs, a relatively small number of circRNA molecules may be sufficient to exert biological functions in the recipient cells. We provide evidence of this, in addition to describing a mechanism in invasive breast cancer cells that can horizontally transmit "advantageous" properties to other cancer cells. The involvement of circSKA3 in cancer cell transmission of functions could also mediate tumor-stromal interactions, providing an approach for cancer cells to modulate stromal cell activities. This could serve as a target for cancer therapy.

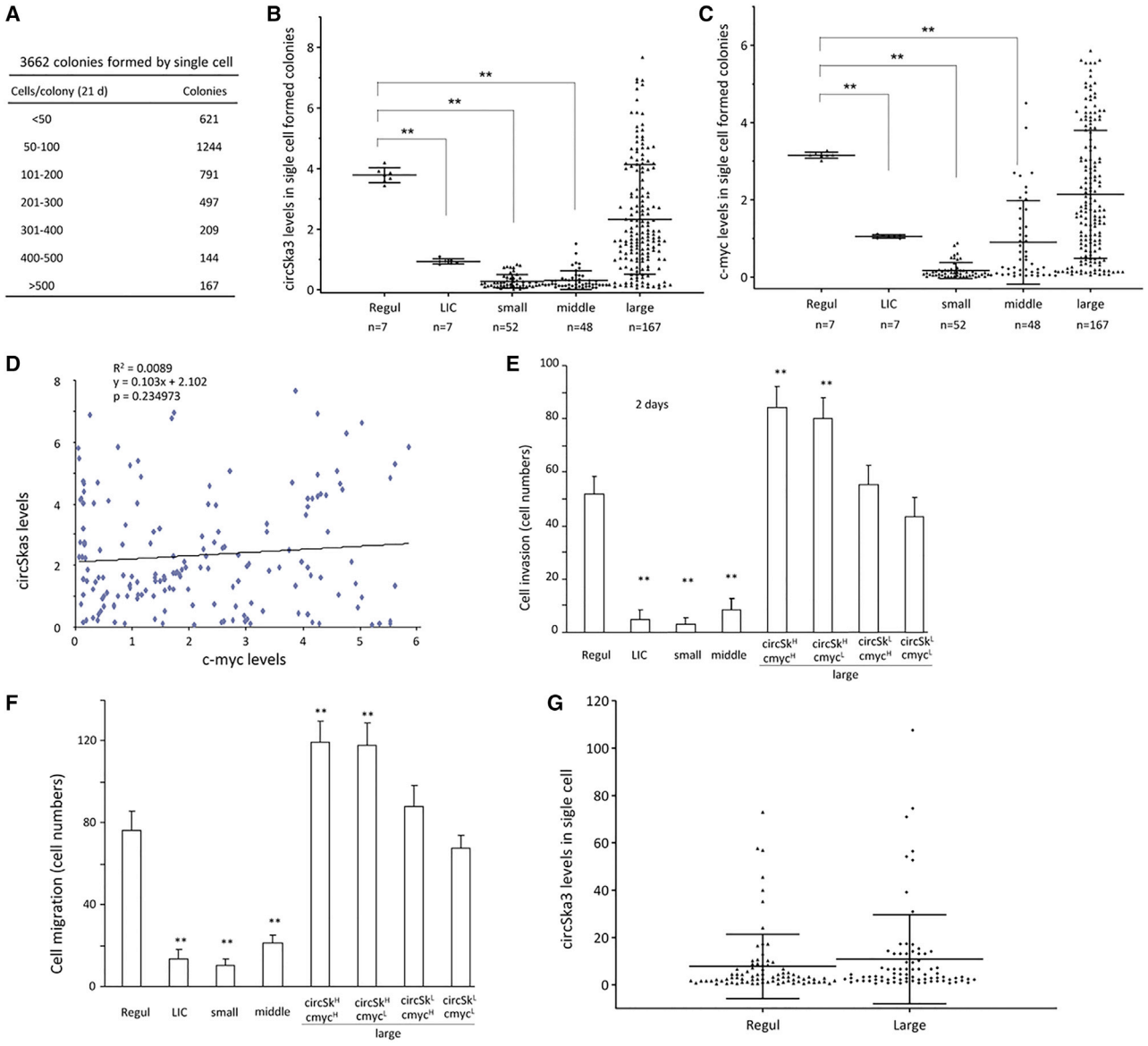

Figure 7. Heterogeneity of circSKA3 expression

(A) Single-cell colonies were obtained and counted after 3 weeks of culture. (B) At least 200 cells were collected and pooled into one sample (n = 1) from small colonies (containing less than 50 cells; n = 52), regular culture (Regul; n = 7), low-invasion colonies (LICs; n = 7), middle colonies (200–300 cells; n = 48), and large colonies (>500 cells; n = 167). All samples were processed to real-time PCR. LICs and small and middle colonies showed decreased circSKA3 levels. (C) LICs and small and middle colonies also showed decreased c-myc levels. (D) Levels of circSKA3 and c-myc in 167 large colonies were not correlated. (E) In a cell invasion assay, each Matrigel-coated chamber insert was loaded with 200 cells harvested from regular colonies, LICs, and small, middle, and large colonies (n = 4). All large colonies were grouped into circSKA3^{H}/c-myc^{H}, circSKA3^{H}/c-myc^{L}, circSKA3^{L}/c-myc^{H}, and circSKA3^{L}/c-myc^{L}. LIC and small- and middle-colony cells showed a decreased invasion ability, while circSKA3^{H} colonies showed an enhanced invasion. (F) In cell migration assays, large colonies with high levels of circSKA3, but not c-myc, promoted cell activities. (G) The large-colony cells (circSKA3^{H}/c-myc^{H}) were subjected to single-cell PCR to measure circSKA3 levels. A similar pattern of circSKA3 distribution was observed in the regular culture. ** p<0.01; Error bars, SD

In the two models used to explain cancer heterogeneity, the CSC model relies on the detection of CSC markers. CSCs can self-renew and differentiate into non-CSCs, and only the self-renewed CSCs retain cancer-developing potential. We found that cells with a low invasive ability can acquire an invasive ability after a co-culture with cells that have a high invasive ability and have obtained a regular pattern of the invasive cancer cells as a result of circSKA3 transmission through exosomes. Our results suggest that the stemless cells

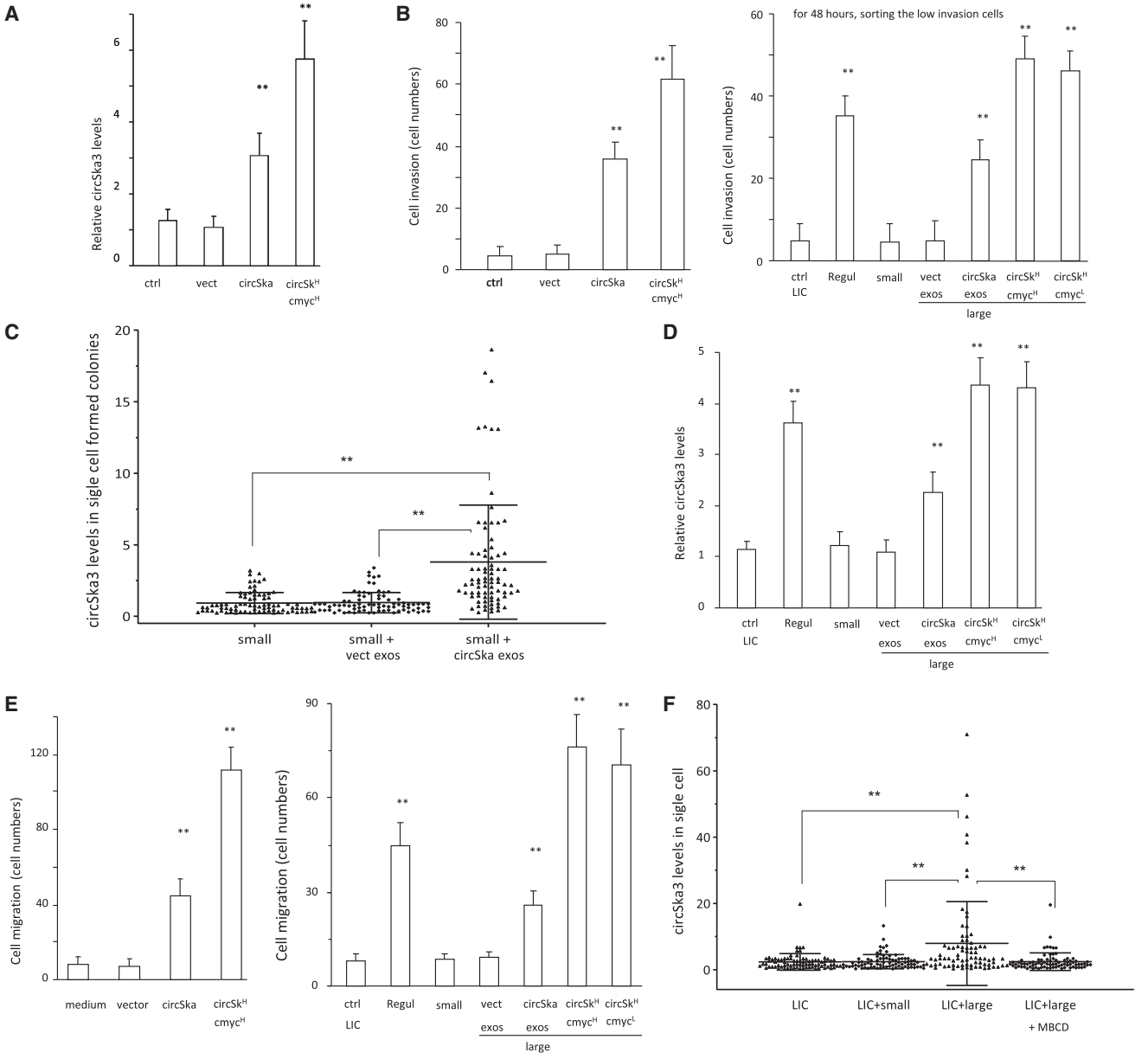

Figure 8. Transfer of circSKA3 potentiates cell invasion

(A) Small-colony cells (n = 4) were cultured with a basal medium, vectored packed exosomes, and circSKA3 packed exosomes (100 ug/mL) for 3 days, and the medium was changed every 8 h. Small-colony cells showed increased circSKA3 levels after circSKA3-packed exosome treatment. However, they still showed lower circSKA3 levels than large-colony cells (circSKA3H/c-mycH group; n = 4). (B) Left, circSKA3-packed exosome treatment increased small-colony cell invasion. Right, LICs showed a promoted invasion ability after being co-cultured with large-colony cells (n = 4). (C) Small-colony cells were co-cultured without or with exosomes purified from the vector- or circSKA3-transfected cells. Treatment with exosomes from the circSKA3 cells increased circSKA3 levels . (D) 1,000 LICs were co-cultured with 200 LICs, regular culture cells, small-colony cells, and large-colony cells (circSKA3^{H}/c-myc^{H} and circSKA3^{H}/c-myc^{L}). All of these 200 cultured cells were stably transfected with GFP. After 48 h, the no-GFP LICs were sorted by flow cytometry, and 200 cells were processed to real-time PCR (n = 4). LICs showed increased circSKA3 after being co-cultured with large-colony cells. (E) Left, a co-culture with cells expressing high levels of circSKA3 increased the quantity of circSKA3 tumor cell migration. Right, LICs displayed promoted cell migration after being co-cultured with large-colony cells (n = 4). (F) LICs were co-cultured with small-colony cells, large-colony cells (circSKA3^{H}/c-myc^{H}), and LICs co-cultured with large-colony cells and MβCD. Treatment with large-colony cells increased levels of circSKA3 and resulted in a similar pattern as in the regular cells, which could be blocked by MβCD. ** p<0.01; Error bars, SD

can obtain stem properties epigenetically, although there only exists a small number of these stem-potential cells in a cancer cell population. Our results provide insight into how CSCs regulate the activities of other cancer cells in the same population.

In the clonal evolution model, tumors are initiated from a single cell mutation.[39] The mutation accumulates over the course of tumor progression. In our experimental model, cell populations developed from one single cell are not supposed to acquire many mutations within a short period of time. In addition, after re-culture, only a small number of cells retained the stem potential. These daughter cells showed significant heterogeneity in cancer-developing potential. Our results suggest that the change in stemness is not due to mutations occurring in the small number of cells with cancer stem potential.

Our results suggest that most, if not all, cancer cells have the potential to develop into a new tumor mass. Each of these cells play a distinct role in regulating the malignancy of the tumor population. For example, one or several cells from the population are responsible for generating an oncogenic component such as circSKA3 that can then be delivered to other cells by exosomes. Some cells are responsible for generating other oncogenic components such as c-myc, to be delivered by exosomes to the rest of the cell population, and so on. In our model, most cancer cells have the "stem" potential. The tumor populations try to maintain the heterogeneity rather than quickly accumulate further heterogeneity in a relatively stationary state. However, there is never a truly stationary state between the tumor and the host. Thus, minor dynamic heterogeneity would occur all of the time, but significant heterogeneity will occur when the epigenetic conditions change rapidly, such as during chemotherapies or surgeries. In these cases, the tumor population will develop further heterogeneity to adapt to the new environment. The inherent heterogeneity of cancer cells underlies the evolution of tumor cells and the potential for resistance to medical treatments. We show that, using exosomes, cancer cells may transfer circRNA and their bound proteins as a strategy to maintain invasive sub-clones. This represents an intriguing avenue necessitating further study for cancer treatment. Thus, our results showed that the heterogeneously expressed circRNA circSKA3 is complexed with integrin β1 and TKS5 to form exosomes. circSKA3 can be transmitted via tumor-derived exosomes to potentiate the invasive potential of breast cancer cells expressing lower levels of circSKA3. Transmission of circSKA3 allows for the maintenance of advantageous invasive sub-clones in breast cancer.

MATERIALS AND METHODS

Cell migration assays

Cell migration was performed by a wound-healing assay and a Transwell chamber assay. In the wound-healing assay, cells were seeded in 6-well plates at a density of 1×10^6 cells/well overnight. To avoid the influence of proliferation, the cells were treated with mitomycin C at 10 μg/mL for 2 h. Cell cultures were scraped linearly with a 200 μL micropipette tip. At different time points, cell locomotion patterns were recorded by an inverted light microscope. The migration distance was measured and quantified. To test cell motility in a three-dimensional way, a polyethylene terephthalate (PET) track membrane (Coster, Sigma-Aldrich) was placed in 24-well tissue culture plates, and 1×10^5 cells in 100 μL media without fetal bovine serum (FBS) were loaded into the upper of the chamber membrane. The lower chamber of the wells was filled with 800 μL DMEM containing 10% FBS. After incubation at 37°C for different time points, non-migrated cells were removed with a cotton swab, and the invaded cells were fixed by 100% methanol for 30 min, followed by staining with Coomassie blue for 10 min. Photos were taken under an inverted light microscope for quantitation. All the migration assays were performed in 2 μg/mL mitomycin C medium. Detailed procedures were provided in our previous publication.[55]

Cell invasion assays

To avoid the influence of proliferation, the cells were treated with mitomycin C at 10 μg/mL for 2 h. circSKA3- and vector-transfected cells were loaded into a serum-free medium with 2 μg/mL mitomycin C inside Transwell inserts. The inserts were pre-coated with 100 mL of Matrigel (diluted at 1:10) and placed in 24-well plates. The chambers of the wells were filled with medium supplemented with 10% FBS and 2 μg/mL mitomycin C. Cells were incubated at 37°C for different time points and allowed to invade and migrate through the Matrigel onto the membrane pores of the inserts. After 48 h, the upper Matrigel layer and cells were removed. The cells that migrated to the surface of the lower side of the membrane were fixed and stained with Coomassie blue for 10 min. Photos were taken under an inverted light microscope for quantitation.

Fluorescence *in situ* hybridization (FISH)

To identify circSKA3 within cells, we performed *in situ* hybridization (FISH) with a Cy5-labelled DNA oligo probe complementary to the junction sequence of circSKA3. A scramble DNA oligo labeled with Cy5 was used as a negative control. Cells were cultured in normal tissue culture slides and fixed with 3.7% formaldehyde for 10 min. The cell membrane was permeabilized with 0.2% Triton X-100 for 15 min. *In situ* hybridization was performed in a hybridization buffer containing 40 nM Cy5-labeled DNA oligo probes at 52°C for 3 h. The slides were subjected to serial washes with saline sodium citrate (SSC) buffers. The slides were then treated with 3% hydrogen peroxide to inactivate endogenous peroxidase activity and washed with a TN buffer (0.1 M Tris-HCl, pH 7.5, and 0.15 M NaCl) three times. The slides were incubated in a blocking buffer (0.1 M Tris-HCl, pH 7.5, 0.15 M NaCl, 0.5% blocking reagent, and 0.5% BSA) at room temperature for 30 min. Genomic DNA was visualized with DAPI. Laser scanning was performed using an LSM 510 Meta confocal microscope (Carl Zeiss) for quantitation.

Tumor formation assay

All mouse experiments were conducted according to the guidelines approved by the Animal Care Committee at Sunnybrook Research Institute (protocol number: AUP 19-076). Mice were kept in the Animal Core Facility of Sunnybrook Research Institute under normal living conditions for 1 week before use. Two types of tumor formation assays were performed.

In assay 1, four-week-old CD-1 nude mice were randomly divided into 5 groups: control, siRNA, RNAse A, MβCD, and Digoxin. Each group had 10 mice. All mice were injected intraperitoneally with MDA-MB-231 cells (5×10^6 cells/mouse). The next day, after cell implantation, circSKA3 siRNA (5 μg/mouse) was conjugated with PEG-Au NP complexes intraperitoneally. This was repeated every 3 days until the experiment was completed. The control group was injected with 0.9% sodium chloride at the same volume on the same schedule. RNAse A (1 μg/mouse) was injected every day, while MβCD (100 μg/mouse) and Digoxin (10 μg/mouse) were injected intraperitoneally with 0.9% sodium chloride at the same volume every 2 days.

In assay 2, four-week-old C57 mice were randomly divided into 5 groups: control, circSKA3, circSKA3 + RNAse A, circSKA3 + MβCD, and circSKA3 + Digoxin. Each group had 15 mice. After injection with B16 cells, the circSKA3 groups were injected intraperitoneally with circSKA3-packed exosomes (500 μg/mouse) daily, while the control group was injected with the control exosomes at the same volume on the same schedule. The control and circSKA3-containing exosomes were extracted from the medium of the vector- and circSKA3-transfected B16 cells.

Western blotting

Western blotting was performed as described.[56,57]

Real-time PCR

Regular, real-time PCR was performed as described.[58] Briefly, total RNA was extracted from tissues or cells using a kit from Geneaid TriRNA isolation kit or TRIzol. 1 μg RNA was used for reverse transcription and real-time PCR using iScript RT kits and SYBR green master mix (Bio-Rad). Primers for U6 or GAPDH were used as internal controls for normalization. The sequences of primers are listed in Table S1.

Single-cell real-time PCR was performed as described.[59] In brief, the cultured cells were trypsinized and suspended in basal medium. A single cell was collected with a glass capillary under an avert phase contrast microscope. After being washed with PBS, the picked cell was lysated with 2 μL lysis buffer (containing 50 mM guanidine thiocyanate, Sigma-Aldrich). All the lysated samples were used to synthesize cDNA with a RT kit in 10 μL. Real-time PCR was performed with a miScriptSYBR GreenPCR Kit (Qigen) using 2 μL cDNA as template. For *in vivo* single-cell real-time PCR, the tumor tissues were washed with PBS, cut into small pieces, and cultured in the basal medium for 12 h. The attached tumor cells were trypsinized and suspended in basal medium. A single cell was collected, lysed, and processed to real-time PCR as above.

Subcellular fractionation

Cultured cells were transferred to a 500 μL fractionation buffer (250 mM sucrose, 20 mM HEPES pH 7.4, 10 mM KCl, 2 mM MgCl2, 1 mM EDTA, and 1 mM EGTA and 1× Roche protease inhibitor cocktail), homogenized by 10 passages through a 25 G needle using a 1 mL syringe, and incubated on ice for 20 min. The nuclear pellet was extracted by centrifugation at 720 × *g* for 5 min. The supernatant was centrifuged again at 10,000 × *g*. The resulting supernatant was centrifuged at 100,000 × *g* for 1 h. The resulting supernatant contained the cytosolic protein fraction. The pellet contained the membrane fraction.

Lipid raft fractionation

The above membrane fractions were lysed in 2 mL of 2-(N-morpholino) ethanesulfonic acid (MES)-buffered saline (MBS: 25 mM MES, 150 mM NaCl, pH 6.0) with protease inhibitors (PIs; Roche Applied Science, Penzberg, Germany) and homogenized with a pre-chilled Dounce homogenizer (Thomas Scientific, Swedesboro, NJ, USA) with 20 strokes. Samples were centrifuged at 1,000 × g for 5 min. The supernatant (2 mL) was adjusted to contain 45% sucrose by adding 2 mL of 90% sucrose in MBS. Following this, 4 mL 35% sucrose in MBS/Na2CO3 (250 mM) and 4 mL 5% sucrose MBS/Na2CO3 were, in turn, layered on top of the supernatant. After centrifugation at 39,000 RPM for 16–10 h in an SW41 rotor (Beckman Instruments, Brea, CA, USA), a light-scattering band at the 5%–35% sucrose interface was collected. Twelve (1 mL) fractions were collected, starting from the top of the gradient. For immunoblotting, an equal amount of total protein from each fraction (25 mg) was analyzed.

Exosome isolation

Exosomes were isolated from ascites and culture media using differential ultracentrifugation as described.[60] Briefly, the ascites or culture media were centrifuged sequentially at 4°C for 10 min at 300 × *g* and 20 min at 2,000 × *g* using TX-400 swinging bucket rotor (Thermo Fisher Scientific) and 30 min at 10,000 × *g* and 2 h at 100,000 × *g* using a Beckman Optima LX-80 ultracentrifuge with 50.1Ti (Beckman Coulter). The pellet was resuspended in PBS and then centrifuged at 100,000 × *g* for 1 h. The pellet was resuspended in PBS and stored at −80°C. Protein contents were measured using a Bio-Rad protein assay kit (BIO-RAD), and total RNAs were determined by Nanodrop (2000) (Thermo, Wilmington, USA).

Exosome RNA immunoprecipitation (RIP) and RNA pull-down assays

Isolated exosomes were lysed in 500 μL coIP buffer and incubated with 5 μg of a primary antibody at 4°C for 2 h. 40 μL of 50% slurry of Protein A-Sepharose was added to each sample, and the mixtures were incubated at 4°C for 4 h. The pellets were washed 3 times with PBS and resuspended in 0.5 mL Tri Reagent (Sigma-Aldrich). The co-precipitated RNA in the aqueous solution was subjected to real-time PCR to analyze the interaction of circRNA with protein precipitated by the antibody. RNA pull-down assays were performed as described.[61]

Invadopodia detection and gelatin degradation assay

An invadopodia gelatin degradation assay was performed as described.[62] Briefly, coverslips were coated with Oregon green 488 conjugated gelatin (0.2 mg/mL)/2.5% sucrose solution in PBS. The gelatin was cross-linked with 0.5% glutaraldehyde and quenched

with 5 mg/mL sodium borohydride. Cells were cultured on the gelatin for 24 h, fixed with 4% paraformaldehyde (PFA), blocked with 3% BSA in PBS, and stained with DAPI (blue) for nuclei and red fluorescence showing F-actin.

Invadopodia isolation

Cells were cultured on gelatin-coated and cross-linked culture dishes and separated into the cytosol fractions, cell body membranes, and invadopodia, as described.[63] Briefly, cells were rinsed in a tyrosine phosphorylated protein (YPP) buffer (10 mM MOPS, pH 6.8, 100 mM KCl, 2.5 mM $MgCl_2$, 1 mM $CaCl_2$, 0.3M sucrose, 1× protease inhibitor cocktail). Cell bodies were sheared with a glass rod into 200 μL YPP buffer. Cell body membranes were separated from the cytosol by centrifugation at 9,000 × *g* at 4°C for 20 min. The invadopodia, embedded in the gelatin matrix, were scraped up together with the cross-linked gelatin and resuspended in coIP buffers.

Single-cell colony culture

The GFP stably transfected MDA-MB-231 cells were inoculated in Petri dishes in DMEM containing 10% FBS, which allowed the cells to attach but not spread as culture plates did. Cells were treated with trypsin/EDTA and quantified by serial dilutions in the next day. Briefly, the cells were diluted to obtain a density of 1 cell per 100 μL and distributed into 96-well tissue culture plates. The cells were observed under a light microscope with fluorescence. Wells that contained one single cell were marked. Wells were excluded if more than one or no growing colonies were detected within 1–2 days. The cells were monitored and photographed, and the cell count was quantified daily until 3 weeks.

Collection of low invasive population cells

MDA-MB-231 cells were cultured on gelatin-coated (0.2 mg/mL) dishes for 48 h. Cells were gently washed with PBS and incubated with 0.025% trypsin/EDTA for 3 s. 10 mL serum-free DMEM was gently filled in the dishes, and the collected floated cells were centrifuged, resuspended, and cultured in 10% FBS/DMEM.

Statistical analysis

All experiments were performed in triplicate. Data were presented as mean (bar) with standard deviation (SD; whisker). For multiple group analyses, a one-way ANOVA followed by a Bonferroni post hoc test for one independent variable were performed. A two-tailed unpaired Student's t test was performed to assess the difference between two groups with a single independent factor. When normal distribution was not confirmed, non-parametric two-tailed unpaired Mann-Whitney or Kruskal-Wallis (followed by Dunn's correction) tests were performed. The levels of significance were set at $^*p < 0.05$ and $^{**}p < 0.01$.

SUPPLEMENTAL INFORMATION

Supplemental information can be found online at https://doi.org/10.1016/j.omtn.2021.11.027.

ACKNOWLEDGMENTS

This work was supported by grants from the Canadian Institutes of Health Research (PJT-153105 and PJT-155962) to B.B.Y. All mouse experiments were approved by the Animal Care Committee at Sunnybrook Research Institute (protocol number: AUP 19-076).

AUTHOR CONTRIBUTIONS

W.W.D., J.M., X.L., N.W., W.Y., F.L., L.F., and P.D. performed the experiments. W.W.D., W.Y., and X.L. initiated the studies. W.W.D. and B.B.Y. analyzed the results. A.J.Y. and B.B.Y. designed and oversaw the project. W.W.D., W.Y., and B.B.Y. wrote the paper.

DECLARATION OF INTEREST

The authors declare no competing interests.

REFERENCES

1. Chen, Y.G., Kim, M.V., Chen, X., Batista, P.J., Aoyama, S., Wilusz, J.E., Iwasaki, A., and Chang, H.Y. (2017). Sensing self and foreign circular RNAs by intron identity. Mol. Cell *67*, 228–238.e5.
2. Zhang, Y., Zhang, X.O., Chen, T., Xiang, J.F., Yin, Q.F., Xing, Y.H., Zhu, S., Yang, L., and Chen, L.L. (2013). Circular intronic long noncoding RNAs. Mol. Cell *51*, 792–806.
3. Li, Z., Huang, C., Bao, C., Chen, L., Lin, M., Wang, X., Zhong, G., Yu, B., Hu, W., Dai, L., et al. (2015). Exon-intron circular RNAs regulate transcription in the nucleus. Nat. Struct. Mol. Biol. *22*, 256–264.
4. Hansen, T.B., Jensen, T.I., Clausen, B.H., Bramsen, J.B., Finsen, B., Damgaard, C.K., and Kjems, J. (2013). Natural RNA circles function as efficient microRNA sponges. Nature *495*, 384–388.
5. Jeck, W.R., Sorrentino, J.A., Wang, K., Slevin, M.K., Burd, C.E., Liu, J., Marzluff, W.F., and Sharpless, N.E. (2013). Circular RNAs are abundant, conserved, and associated with ALU repeats. RNA *19*, 141–157.
6. Memczak, S., Jens, M., Elefsinioti, A., Torti, F., Krueger, J., Rybak, A., Maier, L., Mackowiak, S.D., Gregersen, L.H., Munschauer, M., et al. (2013). Circular RNAs are a large class of animal RNAs with regulatory potency. Nature *495*, 333–338.
7. Zheng, Q., Bao, C., Guo, W., Li, S., Chen, J., Chen, B., Luo, Y., Lyu, D., Li, Y., Shi, G., et al. (2016). Circular RNA profiling reveals an abundant circHIPK3 that regulates cell growth by sponging multiple miRNAs. Nat. Commun. *7*, 11215.
8. Rybak-Wolf, A., Stottmeister, C., Glazar, P., Jens, M., Pino, N., Giusti, S., Hanan, M., Behm, M., Bartok, O., Ashwal-Fluss, R., et al. (2015). Circular RNAs in the mammalian brain are highly abundant, conserved, and dynamically expressed. Mol. Cell *58*, 870–885.
9. Legnini, I., Di Timoteo, G., Rossi, F., Morlando, M., Briganti, F., Sthandier, O., Fatica, A., Santini, T., Andronache, A., Wade, M., et al. (2017). Circ-ZNF609 is a circular RNA that can be translated and functions in myogenesis. Mol. Cell *66*, 22–37.e9.
10. Tatomer, D.C., and Wilusz, J.E. (2017). An unchartered journey for ribosomes: circumnavigating circular RNAs to produce proteins. Mol. Cell *66*, 1–2.
11. Wang, J., Zhu, S., Meng, N., He, Y., Lu, R., and Yan, G.R. (2019). ncRNA-encoded peptides or proteins and cancer. Mol. Ther. *27*, 1718–1725.
12. Du, W.W., Xu, J., Yang, W., Wu, N., Li, F., Zhou, L., Wang, S., Li, X., He, A.T., Du, K.Y., et al. (2021). A neuroligin isoform translated by circNlgn contributes to cardiac remodeling. Circ. Res. *129*, 568–582.
13. Santer, L., Bar, C., and Thum, T. (2019). Circular RNAs: a novel class of functional RNA molecules with a therapeutic perspective. Mol. Ther. *27*, 1350–1363.
14. Zhou, Z.B., Huang, G.X., Fu, Q., Han, B., Lu, J.J., Chen, A.M., and Zhu, L. (2019). circRNA.33186 contributes to the pathogenesis of osteoarthritis by sponging miR-127-5p. Mol. Ther. *27*, 531–541.
15. Zhu, K.P., Zhang, C.L., Ma, X.L., Hu, J.P., Cai, T., and Zhang, L. (2019). Analyzing the interactions of mRNAs and ncRNAs to predict competing endogenous RNA networks in osteosarcoma chemo-resistance. Mol. Ther. *27*, 518–530.

16. Du, W.W., Fang, L., Yang, W., Wu, N., Awan, F.M., Yang, Z., and Yang, B.B. (2017). Induction of tumor apoptosis through a circular RNA enhancing Foxo3 activity. Cell Death Differ. *24*, 357–370.

17. Du, W.W., Yang, W., Chen, Y., Wu, Z.K., Foster, F.S., Yang, Z., Li, X., and Yang, B.B. (2017). Foxo3 circular RNA promotes cardiac senescence by modulating multiple factors associated with stress and senescence responses. Eur. Heart J. *38*, 1402–1412.

18. Du, W.W., Yang, W., Liu, E., Yang, Z., Dhaliwal, P., and Yang, B.B. (2016). Foxo3 circular RNA retards cell cycle progression via forming ternary complexes with p21 and CDK2. Nucleic Acids Res. *44*, 2846–2858.

19. Du, W.W., Zhang, C., Yang, W., Yong, T., Awan, F.M., and Yang, B.B. (2017). Identifying and characterizing circRNA-protein interaction. Theranostics *7*, 4183–4191.

20. Sang, Y., Chen, B., Song, X., Li, Y., Liang, Y., Han, D., Zhang, N., Zhang, H., Liu, Y., Chen, T., et al. (2019). circRNA_0025202 regulates tamoxifen sensitivity and tumor progression via regulating the miR-182-5p/FOXO3a axis in breast cancer. Mol. Ther. *27*, 1638–1652.

21. Fang, L., Du, W.W., Awan, F.M., Dong, J., and Yang, B.B. (2019). The circular RNA circ-Ccnb1 dissociates Ccnb1/Cdk1 complex suppressing cell invasion and tumorigenesis. Cancer Lett. *459*, 216–226.

[22]. Zhou, C., Liu, H.S., Wang, F.W., Hu, T., Liang, Z.X., Lan, N., et al. (2020). circCAMSAP1 promotes tumor growth in colorectal cancer via the miR-328-5p/E2F1 axis. Mol. Ther. *28*, 914–928.

23. Chen, Y., Yang, F., Fang, E., Xiao, W., Mei, H., Li, H., Li, D., Song, H., Wang, J., Hong, M., et al. (2019). Circular RNA circAGO2 drives cancer progression through facilitating HuR-repressed functions of AGO2-miRNA complexes. Cell Death Differ. *26*, 1346–1364.

24. Sun, Y., Zhang, S., Yue, M., Li, Y., Bi, J., and Liu, H. (2019). Angiotensin II inhibits apoptosis of mouse aortic smooth muscle cells through regulating the circNRG-1/miR-193b-5p/NRG-1 axis. Cell Death Dis. *10*, 362.

25. Du, W.W., Yang, W., Li, X., Fang, L., Wu, N., Li, F., Chen, Y., He, Q., Liu, E., Yang, Z., et al. (2020). The circular RNA circSKA3 binds integrin beta1 to induce invadopodium formation enhancing breast cancer invasion. Mol. Ther. *28*, 1287–1298.

26. Ma, J., Du, W.W., Zeng, K., Wu, N., Fang, L., Lyu, J., Yee, A.J., and Yang, B.B. (2021). An antisense circular RNA circSCRIB enhances cancer progression by suppressing parental gene splicing and translation. Mol. Ther. *29*, 2754–2768.

27. Zhou, L.Y., Zhai, M., Huang, Y., Xu, S., An, T., Wang, Y.H., Zhang, R.C., Liu, C.Y., Dong, Y.H., Wang, M., et al. (2019). The circular RNA ACR attenuates myocardial ischemia/reperfusion injury by suppressing autophagy via modulation of the Pink1/FAM65B pathway. Cell Death Differ. *26*, 1299–1315.

28. Yang, Z.G., Awan, F.M., Du, W.W., Zeng, Y., Lyu, J., Wu, D., Gupta, S., Yang, W., and Yang, B.B. (2017). The circular RNA interacts with STAT3, increasing its nuclear translocation and wound repair by modulating Dnmt3a and miR-17 function. Mol. Ther. *25*, 2062–2074.

29. Wu, N., Yuan, Z., Du, K.Y., Fang, L., Lyu, J., Zhang, C., He, A., Eshaghi, E., Zeng, K., Ma, J., et al. (2019). Translation of yes-associated protein (YAP) was antagonized by its circular RNA via suppressing the assembly of the translation initiation machinery. Cell Death Differ. *26*, 2758–2773.

30. Gaitanos, T.N., Santamaria, A., Jeyaprakash, A.A., Wang, B., Conti, E., and Nigg, E.A. (2009). Stable kinetochore-microtubule interactions depend on the Ska complex and its new component Ska3/C13Orf3. EMBO J. *28*, 1442–1452.

31. Wu, Y., Dai, F., Zhang, Y., Zheng, X., Li, L., Zhang, Y., Cao, J., and Gao, W. (2021). miR-1207-5p suppresses laryngeal squamous cell carcinoma progression by downregulating SKA3 and inhibiting epithelial-mesenchymal transition. Mol. Ther. Oncolytics *22*, 152–165.

32. Gao, W., Zhang, Y., Luo, H., Niu, M., Zheng, X., Hu, W., Cui, J., Xue, X., Bo, Y., Dai, F., et al. (2020). Targeting SKA3 suppresses the proliferation and chemoresistance of laryngeal squamous cell carcinoma via impairing PLK1-AKT axis-mediated glycolysis. Cell Death Dis. *11*, 919.

33. Li, B., Cai, X., Wang, Y., Zhu, H., Zhang, P., Jiang, P., Yang, X., Sun, J., Hong, L., and Shao, L. (2021). Circ-SKA3 enhances doxorubicin toxicity in AC16 cells through miR-1303/TLR4 axis. Int. Heart J. *62*, 1112–1123.

34. Zhao, X., Guan, J., and Luo, M. (2021). Circ-SKA3 upregulates ID3 expression by decoying miR-326 to accelerate the development of medulloblastoma. J. Clin. Neurosci. *86*, 87–96.

35. Shackleton, M., Quintana, E., Fearon, E.R., and Morrison, S.J. (2009). Heterogeneity in cancer: cancer stem cells versus clonal evolution. Cell *138*, 822–829.

36. Singh, S.K., Hawkins, C., Clarke, I.D., Squire, J.A., Bayani, J., Hide, T., Henkelman, R.M., Cusimano, M.D., and Dirks, P.B. (2004). Identification of human brain tumour initiating cells. Nature *432*, 396–401.

37. Lapidot, T., Sirard, C., Vormoor, J., Murdoch, B., Hoang, T., Caceres-Cortes, J., Minden, M., Paterson, B., Caligiuri, M.A., and Dick, J.E. (1994). A cell initiating human acute myeloid leukaemia after transplantation into SCID mice. Nature *367*, 645–648.

38. Shipitsin, M., Campbell, L.L., Argani, P., Weremowicz, S., Bloushtain-Qimron, N., Yao, J., Nikolskaya, T., Serebryiskaya, T., Beroukhim, R., Hu, M., et al. (2007). Molecular definition of breast tumor heterogeneity. Cancer Cell *11*, 259–273.

39. Nowell, P.C. (1976). The clonal evolution of tumor cell populations. Science *194*, 23–28.

40. Merlo, L.M., Pepper, J.W., Reid, B.J., and Maley, C.C. (2006). Cancer as an evolutionary and ecological process. Nat. Rev. Cancer *6*, 924–935.

41. Jiang, K., Yang, J., Guo, S., Zhao, G., Wu, H., and Deng, G. (2019). Peripheral circulating exosome-mediated delivery of miR-155 as a novel mechanism for acute lung inflammation. Mol. Ther. *27*, 1758–1771.

42. Zhang, D., Lee, H., Wang, X., Rai, A., Groot, M., and Jin, Y. (2018). Exosome-mediated small RNA delivery: a novel therapeutic approach for inflammatory lung responses. Mol. Ther. *26*, 2119–2130.

43. Zhou, C., Zhang, Y., Yan, R., Huang, L., Mellor, A.L., Yang, Y., Chen, X., Wei, W., Wu, X., Yu, L., et al. (2021). Exosome-derived miR-142-5p remodels lymphatic vessels and induces Ido to promote immune privilege in the tumour microenvironment. Cell Death Differ. *28*, 715–729.

44. Deng, T., Zhang, H., Yang, H., Wang, H., Bai, M., Sun, W., Wang, X., Si, Y., Ning, T., Zhang, L., et al. (2020). Exosome miR-155 derived from gastric carcinoma promotes angiogenesis by targeting the c-MYB/VEGF axis of endothelial cells. Mol. Ther. Nucleic Acids *19*, 1449–1459.

45. Nakamura, Y., Kita, S., Tanaka, Y., Fukuda, S., Obata, Y., Okita, T., Nishida, H., Takahashi, Y., Kawachi, Y., Tsugawa-Shimizu, Y., et al. (2020). Adiponectin stimulates exosome release to enhance mesenchymal stem-cell-driven therapy of heart failure in mice. Mol. Ther. *28*, 2203–2219.

46. Wang, H., Wang, B., Zhang, A., Hassounah, F., Seow, Y., Wood, M., Ma, F., Klein, J.D., Price, S.R., and Wang, X.H. (2019). Exosome-mediated miR-29 transfer reduces muscle atrophy and kidney fibrosis in mice. Mol. Ther. *27*, 571–583.

47. Sun, X., Lin, F., Sun, W., Zhu, W., Fang, D., Luo, L., Li, S., Zhang, W., and Jiang, L. (2021). Exosome-transmitted miRNA-335-5p promotes colorectal cancer invasion and metastasis by facilitating EMT via targeting RASA1. Mol. Ther. Nucleic Acids *24*, 164–174.

48. Yue, Y., Wang, C., Benedict, C., Huang, G., Truongcao, M., Roy, R., Cimini, M., Garikipati, V.N.S., Cheng, Z., Koch, W.J., et al. (2020). Interleukin-10 deficiency alters endothelial progenitor cell-derived exosome reparative effect on myocardial repair via integrin-linked kinase enrichment. Circ. Res. *126*, 315–329.

49. Jiang, K., Dong, C., Yin, Z., Li, R., Mao, J., Wang, C., Zhang, J., Gao, Z., Liang, R., Wang, Q., et al. (2020). Exosome-derived ENO1 regulates integrin alpha6beta4 expression and promotes hepatocellular carcinoma growth and metastasis. Cell Death Dis. *11*, 972.

50. Hoshino, A., Costa-Silva, B., Shen, T.L., Rodrigues, G., Hashimoto, A., Tesic Mark, M., Molina, H., Kohsaka, S., Di Giannatale, A., Ceder, S., et al. (2015). Tumour exosome integrins determine organotropic metastasis. Nature *527*, 329–335.

51. Li, Y., Zheng, Q., Bao, C., Li, S., Guo, W., Zhao, J., Chen, D., Gu, J., He, X., and Huang, S. (2015). Circular RNA is enriched and stable in exosomes: a promising biomarker for cancer diagnosis. Cell Res. *25*, 981–984.

52. Thomou, T., Mori, M.A., Dreyfuss, J.M., Konishi, M., Sakaguchi, M., Wolfrum, C., Rao, T.N., Winnay, J.N., Garcia-Martin, R., Grinspoon, S.K., et al. (2017). Adipose-derived circulating miRNAs regulate gene expression in other tissues. Nature *542*, 450–455.

53. Zhang, L., Zhang, S., Yao, J., Lowery, F.J., Zhang, Q., Huang, W.C., Li, P., Li, M., Wang, X., Zhang, C., et al. (2015). Microenvironment-induced PTEN loss by exosomal microRNA primes brain metastasis outgrowth. Nature *527*, 100–104.

54. Zhang, Y., Kim, M.S., Jia, B., Yan, J., Zuniga-Hertz, J.P., Han, C., and Cai, D. (2017). Hypothalamic stem cells control ageing speed partly through exosomal miRNAs. Nature *548*, 52–57.

55. Du, W.W., Yang, B.B., Shatseva, T.A., Yang, B.L., Deng, Z., Shan, S.W., Lee, D.Y., Seth, A., and Yee, A.J. (2010). Versican G3 promotes mouse mammary tumor cell growth, migration, and metastasis by influencing EGF receptor signaling. PLoS One *5*, e13828.

56. Zhang, Y., Cao, L., Kiani, C., Yang, B.L., Hu, W., and Yang, B.B. (1999). Promotion of chondrocyte proliferation by versican mediated by G1 domain and EGF-like motifs. J. Cell. Biochem. *73*, 445–457.

57. Zhang, Y., Wu, Y., Cao, L., Lee, V., Chen, L., Lin, Z., Kiani, C., Adams, M.E., and Yang, B.B. (2001). Versican modulates embryonic chondrocyte morphology via the epidermal growth factor-like motifs in G3. Exp. Cell Res. *263*, 33–42.

58. Rutnam, Z.J., Du, W.W., Yang, W., Yang, X., and Yang, B.B. (2014). The pseudogene TUSC2P promotes TUSC2 function by binding multiple microRNAs. Nat. Commun. *5*, 2914.

59. Stahlberg, A., and Bengtsson, M. (2010). Single-cell gene expression profiling using reverse transcription quantitative real-time PCR. Methods *50*, 282–288.

60. Liga, A., Vliegenthart, A.D., Oosthuyzen, W., Dear, J.W., and Kersaudy-Kerhoas, M. (2015). Exosome isolation: a microfluidic road-map. Lab Chip *15*, 2388–2394.

61. Wu, N., Xu, J., Du, W.W., Li, X., Awan, F.M., Li, F., Misir, S., Eshaghi, E., Lyu, J., Zhou, L., et al. (2021). YAP circular RNA, circYap, attenuates cardiac fibrosis via binding with tropomyosin-4 and gamma-actin decreasing actin polymerization. Mol. Ther. *29*, 1138–1150.

62. Mader, C.C., Oser, M., Magalhaes, M.A., Bravo-Cordero, J.J., Condeelis, J., Koleske, A.J., and Gil-Henn, H. (2011). An EGFR-Src-Arg-cortactin pathway mediates functional maturation of invadopodia and breast cancer cell invasion. Cancer Res. *71*, 1730–1741.

63. Mueller, S.C., Yeh, Y., and Chen, W.T. (1992). Tyrosine phosphorylation of membrane proteins mediates cellular invasion by transformed cells. J. Cell Biol. *119*, 1309–1325.

OMTN, Volume *27*

Supplemental information

Promotion of tumor progression by exosome transmission of circular RNA circSKA3

William W. Du, Xiangmin Li, Jian Ma, Ling Fang, Nan Wu, Feiya Li, Preet Dhaliwal, Weining Yang, Albert J. Yee, and Burton B. Yang

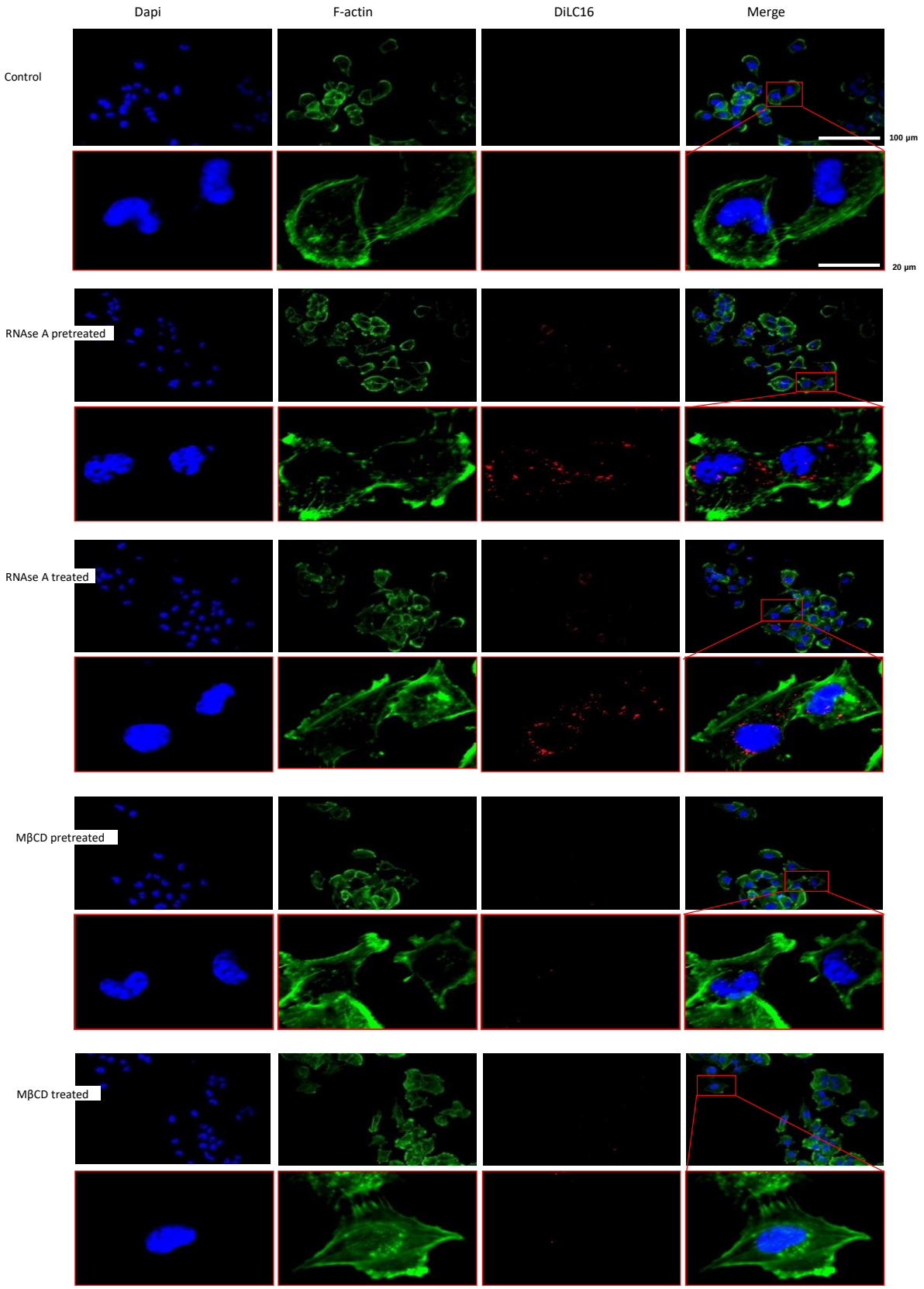

Fig S1. MB-231 cell derived exosomes entered MB-231 cells *in vitro*. Exosomes that were isolated from the medium of DiIC16-labed MB-231 cells (exosome) or, the DiIC16-containing medium without cells (control) and applied to culture MB-231 cells for 24 before detection for fluorescent DiIC16. The RNAse A or MβCD pretreated samples were treated with RNAse A or MβCD during DiIC16 staining, while the RNAse A or MβCD treated cells were cultured with conditioned medium with RNAse A or MβCD for 24 h. Cells were stained with DAPI (blue) for nucleus, green fluorescence showing F-actin, red fluorescence showing DiIC16 (exosome).

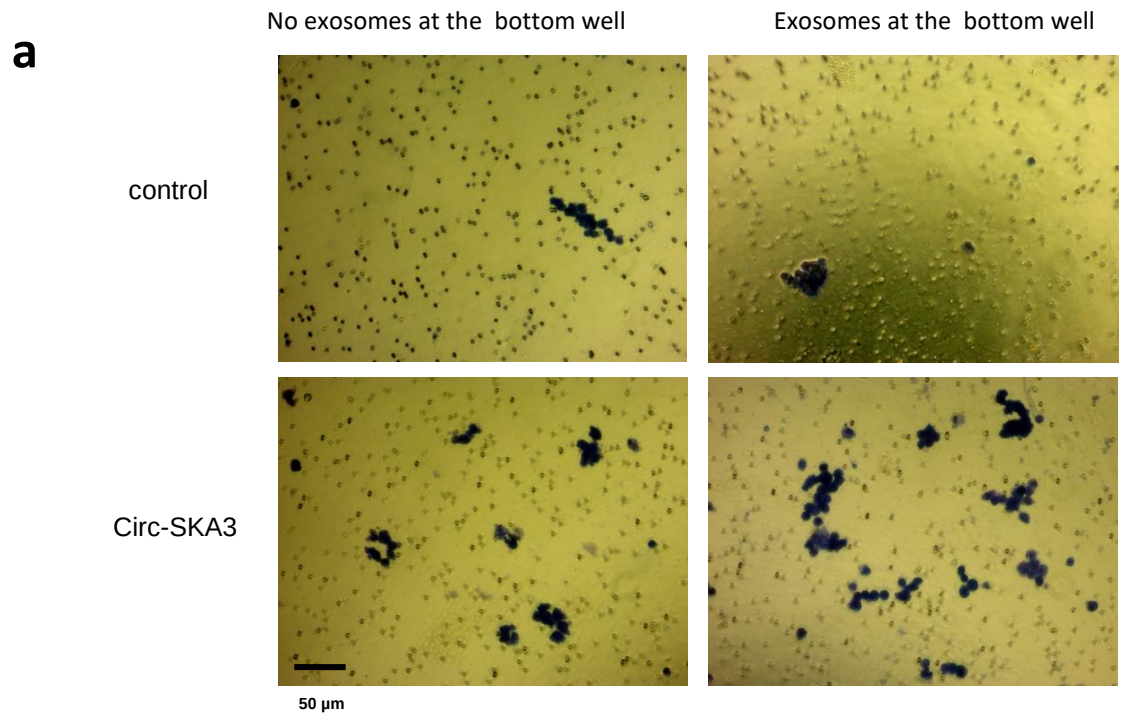

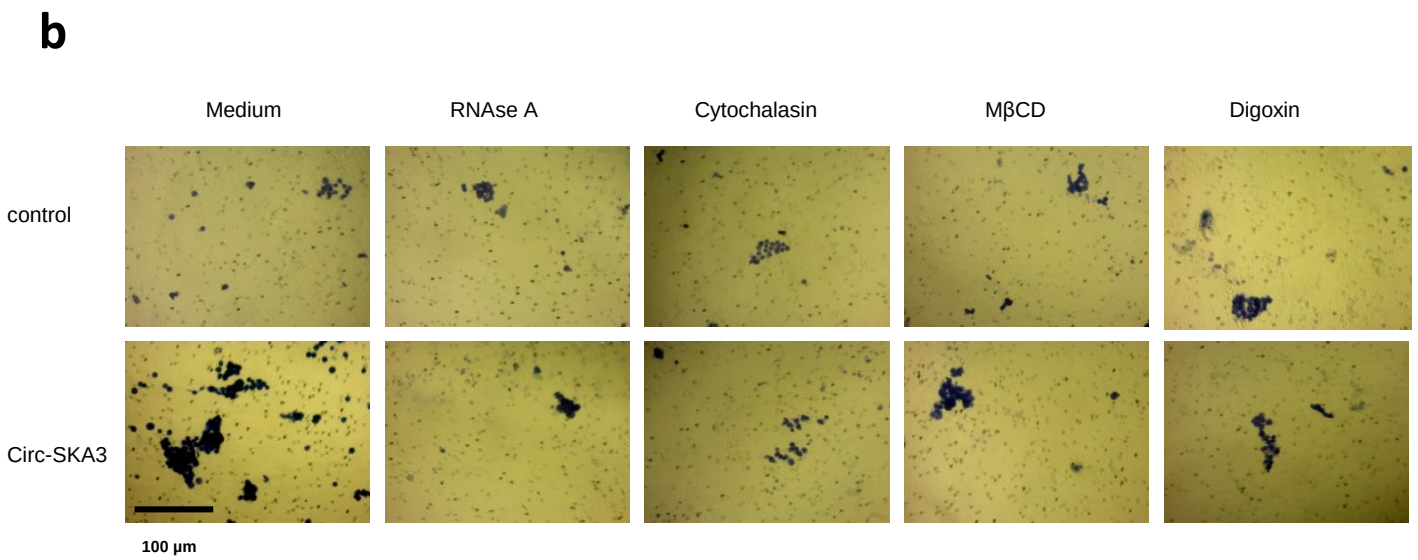

Fig S2. CircSKA3 enhanced cell invasion.
(a) Addition of exosomes containing circSKA3 enhanced MCF-7 cell invasion.
(b) Enhanced invasion of MCF-7 cells was inhibited by RNAse-A, Cytochalasin D, Digoxin and MβCD.

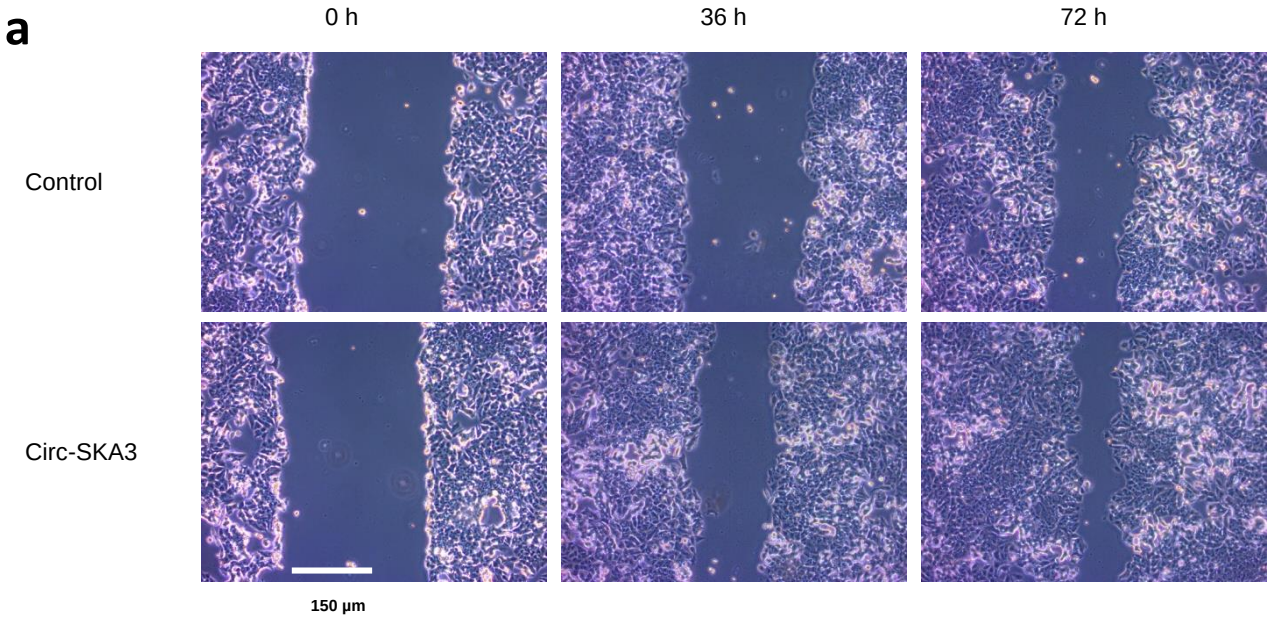

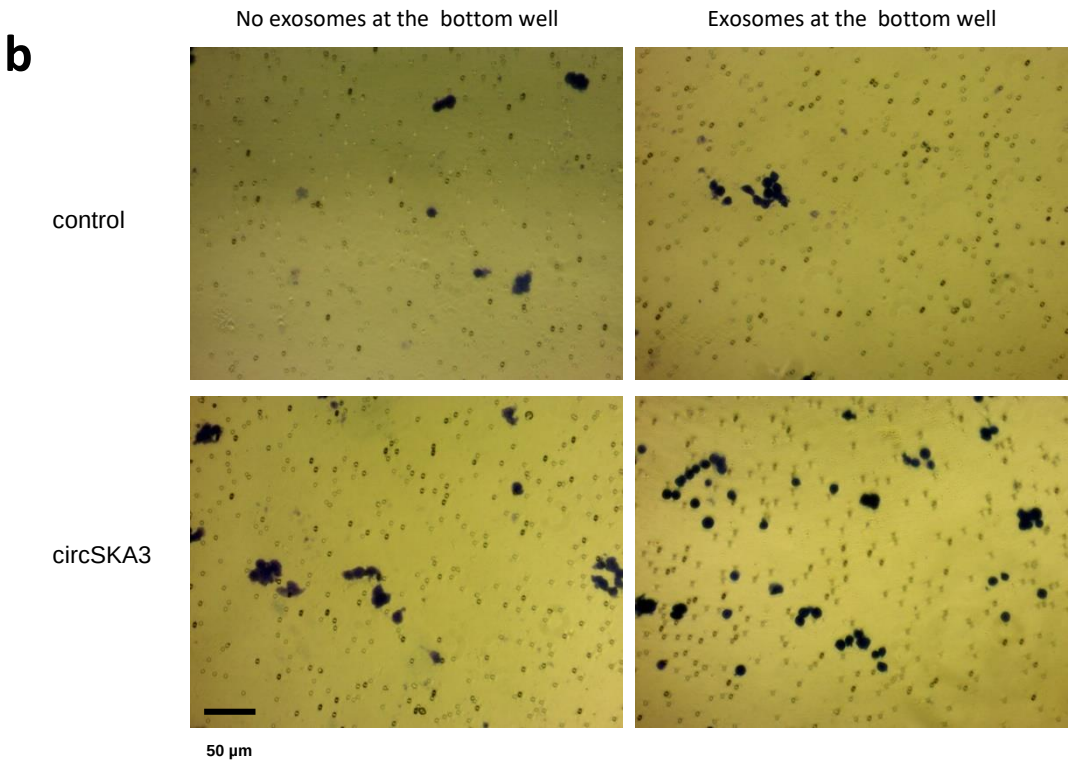

Fig S3. CircSKA3 enhanced cell migration.

(a) MCF-7 cells were culture in basal medium with 100 μg/ml exosomes, and processed to wound healing assays for 3 days. circSKA3-packed exosomes enhanced cell migration.

(b) MCF-7 cells were cultured in basal medium with 100 μg/ml exosomes harvested from vector-, or circSKA3-transfected cells for 3 days. In chamber migration assay, the circSKA3-packed exosomes were placed at the bottom wells. After 3 days, circSKA3-packed exosomes enhanced MCF-7 cell migration.

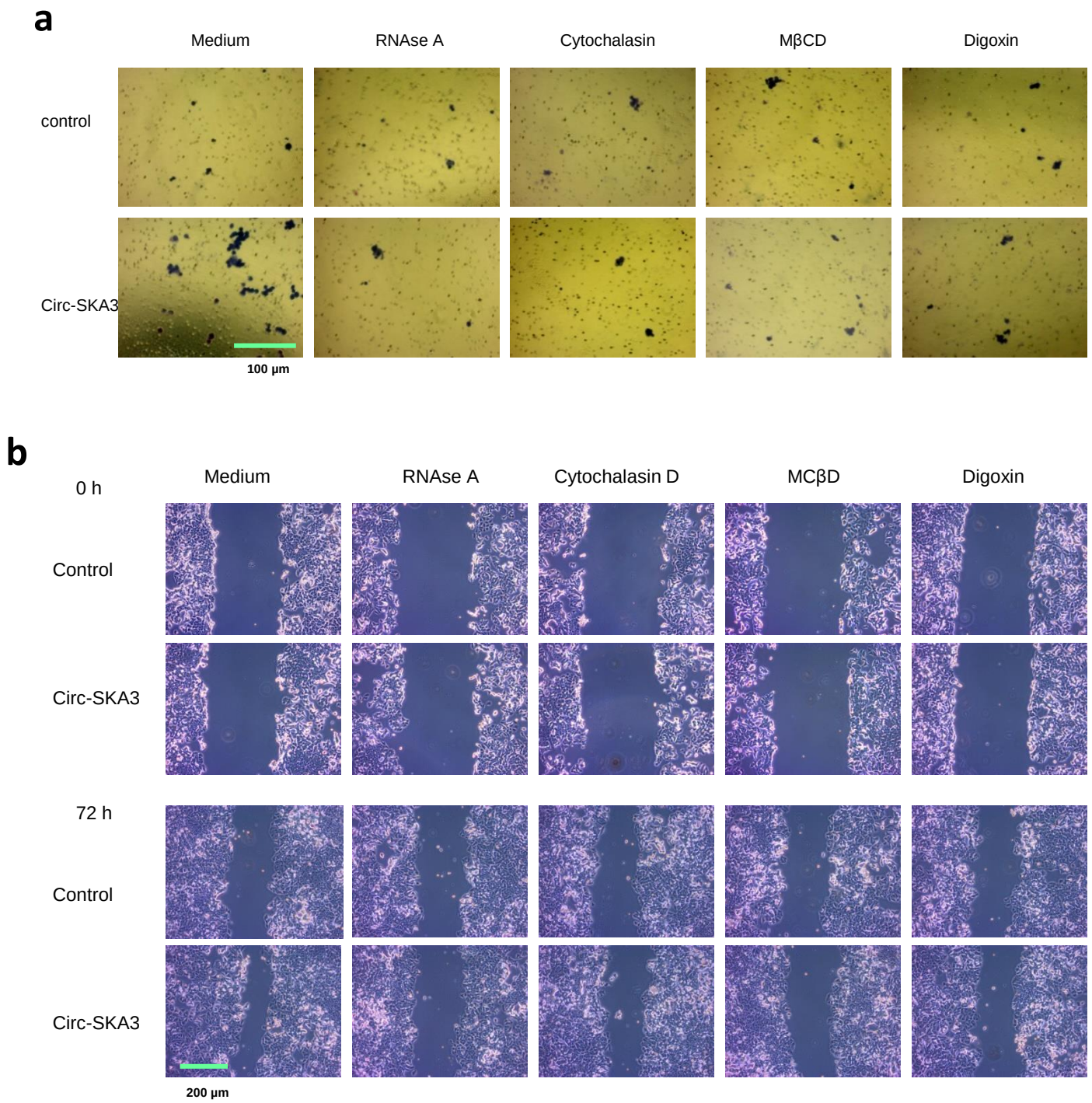

Fig S4. CircSKA3 enhanced cell migration.

(a) MCF-7 cells were culture in basal medium with 100 μg/ml containing vector-, or circSKA3-packed exosomes, to which the chemicals (RNAse-A, Cytochalasin D, Digoxin or MβCD) were added and incubated for 3 days. In the wound healing assays, circSKA3-packed exosomes enhanced cell migration, which could be inhibited by RNAse, Cytochalasin D, Digoxin and MβCD.

(b) In chamber migration assays, enhanced cell migration by circSKA3 was inhibited by RNAse-A, Cytochalasin D, Digoxin and MβCD.

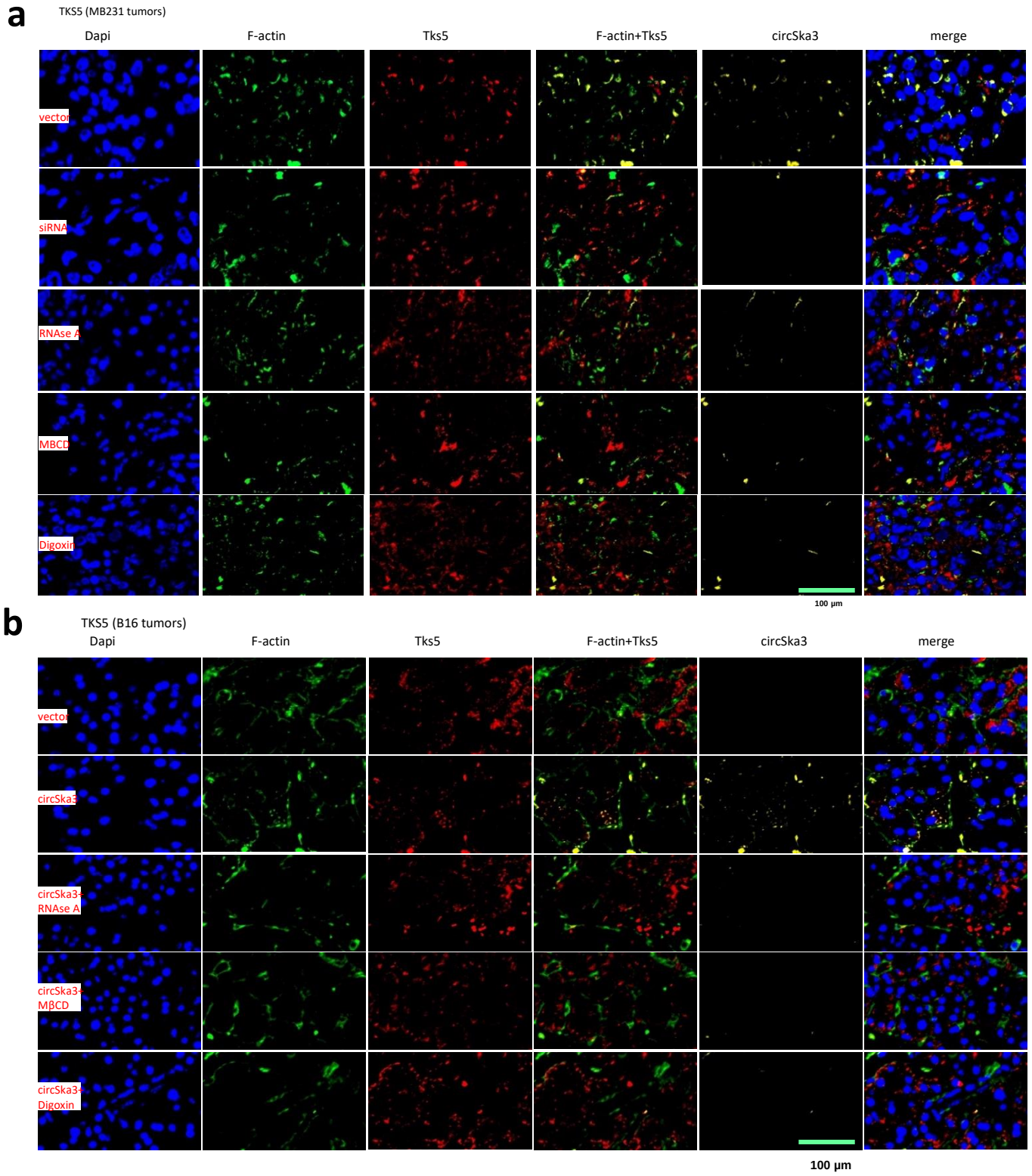

Fig S5. *In vivo* inhibition of exosome transfer.

(a) Invadopodia formation was repressed in the tumor tissues when the mice were injected with circSKA3 siRNA, RNAse A, Methyl-β-cyclodextrin (MβCD), or Digoxin. MB-231 cell formed tumor tissues were stained with DAPI (blue) for nucleus, green fluorescence showing F-actin, red fluorescence showing Tks5, and yellow fluorescence showing circSKA3.

(b) B16 cell formed tumor tissues were stained with DAPI (blue) for nucleus, green fluorescence showing F-actin, red fluorescence showing Tks5, and yellow fluorescence showing circSKA3.

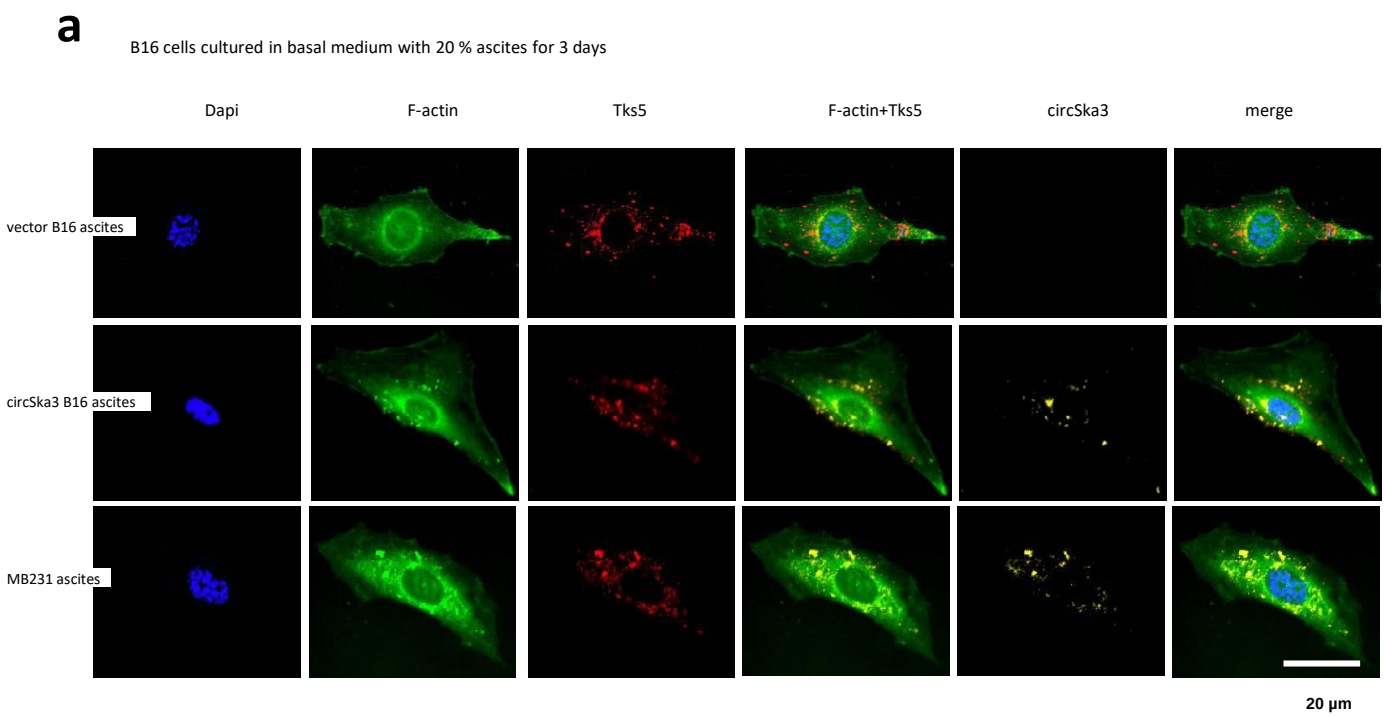

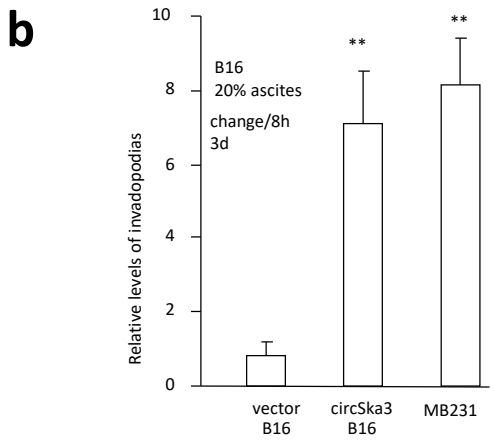

Fig S6. *In vivo* inhibition of exosome transfer.

(a) B16 cells were incubated with basal medium with 20% ascites from B16 cells injected mice, circSKA3 transfected B16 injected mice, or MB-231 cells injected mice for 3 days. Cells were stained with DAPI (blue) for nucleus, green fluorescence showing F-actin, red fluorescence showing Tks5, and yellow fluorescence showing circSKA3. Ascites from circSKA3 transfected B16 or MB-231 cells injected mice enhanced expression of circSKA3 and invadopodia formation.

(b) Image J analysis showed that ascites from mice injected with circSKA3-transfected B16 cells or MB-231 cells promoted invadopodia formation in B16 cells.

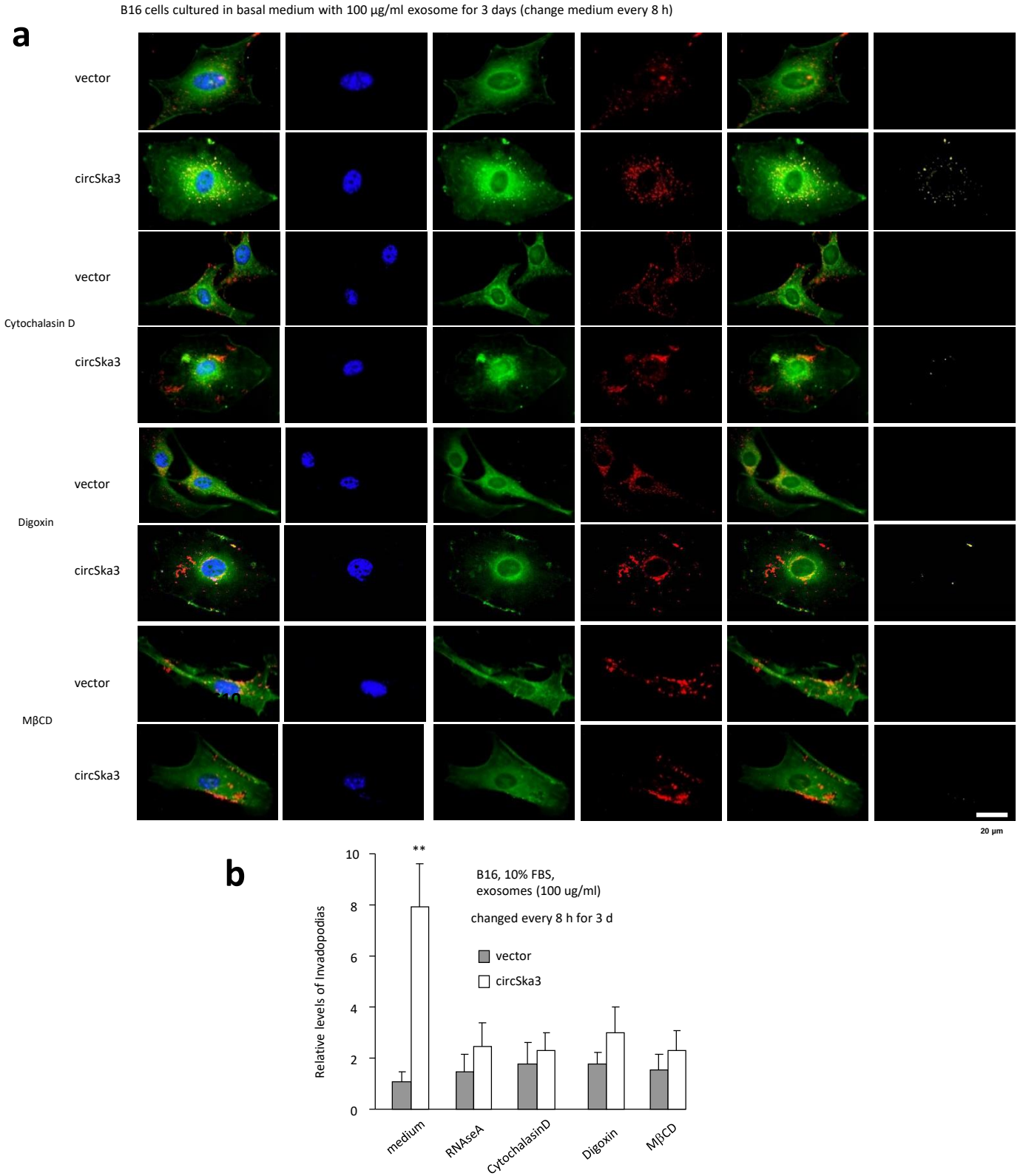

Fig S7. Identification of fractions containing circSKA3 complex.

(a) B16 cells were incubated with 100 μg/ml control vector-, or circSKA3 packed exosomes for 3 days. Cells were stained with DAPI (blue) for nucleus, green fluorescence showing F-actin, red fluorescence showing Tks5, and yellow fluorescence showing circSKA3. circSKA3 packed exosomes enhanced expression of circSKA3 and invadopodia formation in cells, which could be prevented by RNAse, Cytochalasin D, Digoxin and MβCD.

(b) Image J showed that circSKA3-containing exosomes promoted invadopodia formation in B16 cells, which could be prevented by RNAse, Cytochalasin D, Digoxin and MβCD.

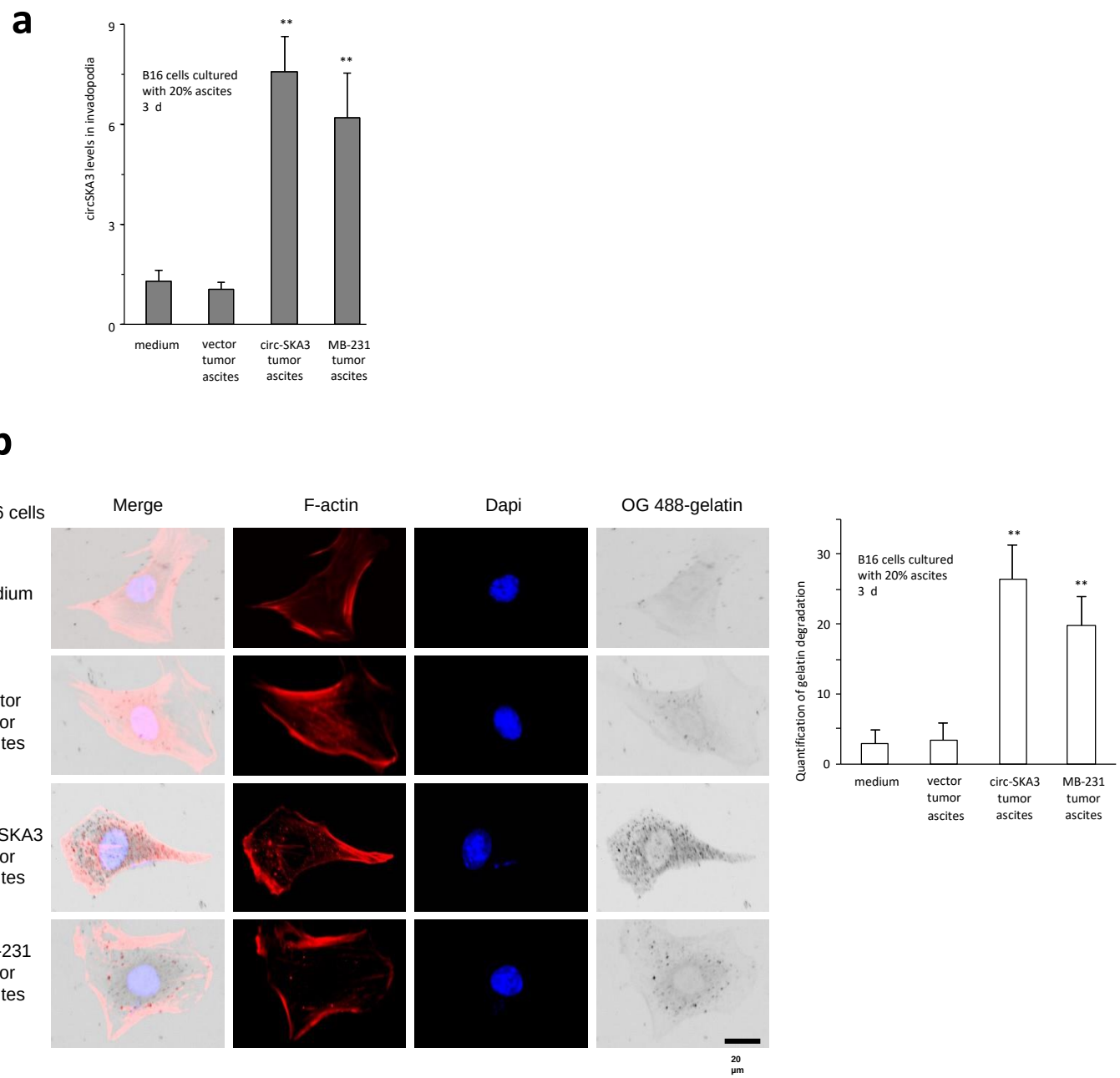

Figure S8. (a) B16 cells were loaded on gelatin coated and crosslinked culture dishes and incubated with basal medium and 20% mouse ascites for 3 days, followed by invadopodia collection and RNA extraction. Ascites from tumor-bearing mice injected with circSKA3-transfected B16 cells or MB-231 cells increased circSKA3 levels in invadopodia of the cultured B16 cells. **, $p<0.01$. Error bars, SD ($n=6$).

(b) B16 cells were incubated with basal medium and 20% mouse ascites for 3 days, followed by gelatin degradation assays (left) and Image-J analysis (right). Ascites from tumor-bearing mice injected with circSKA3-transfected B16 cells or MB-231 cells showed enhanced gelatin degradation. **, $p<0.01$. Error bars, SD ($n=6$).

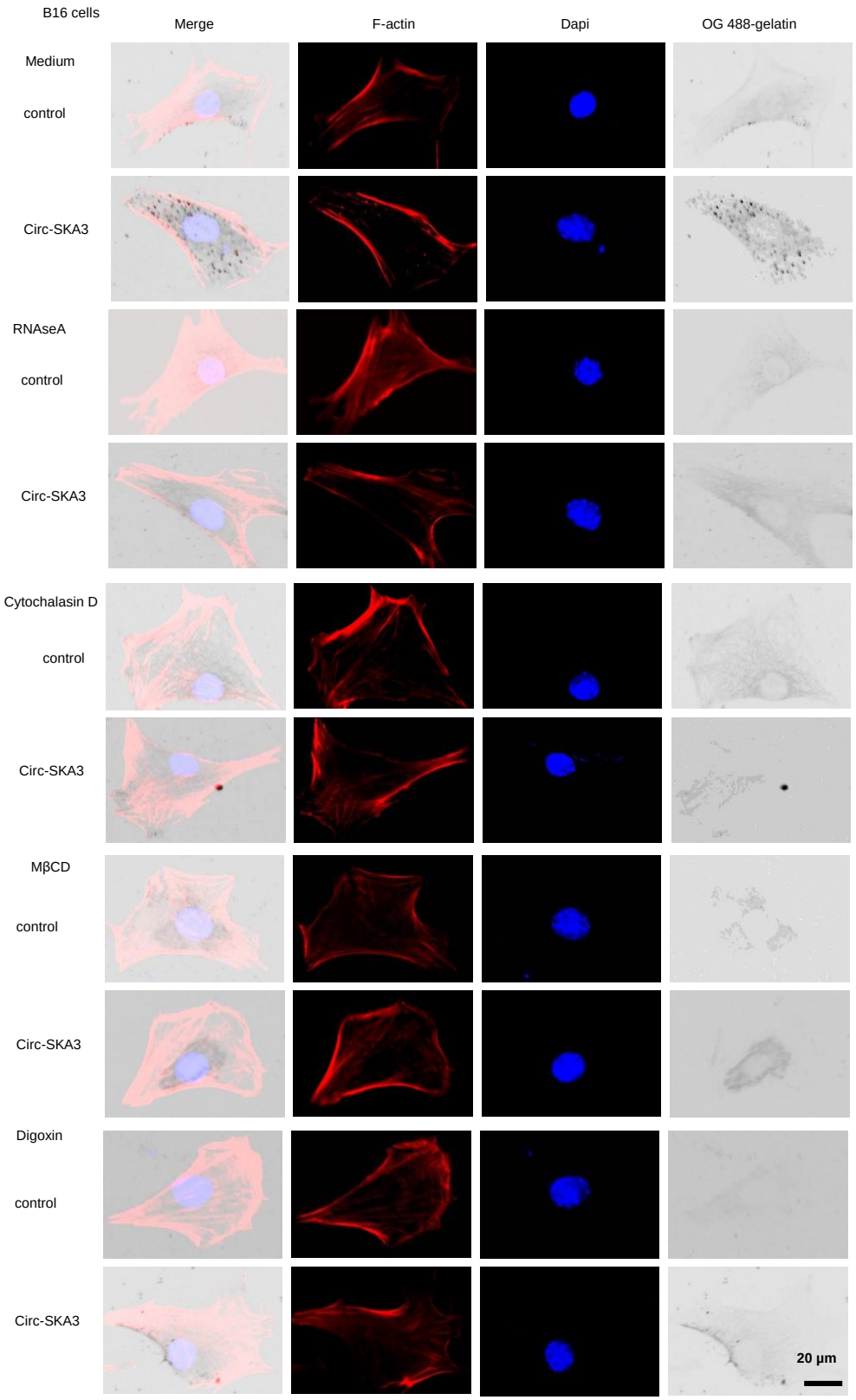

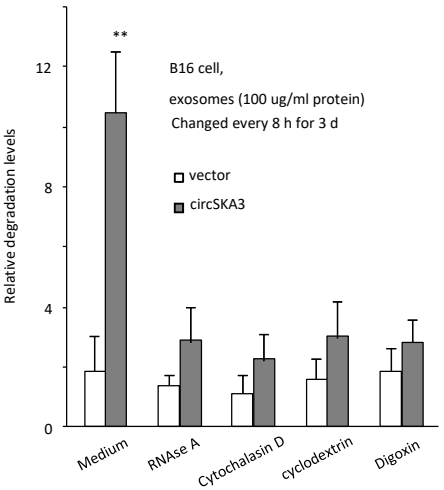

Fig S9. B16 cells were cultured in basal medium with 100 μg/ml control vector-, or circSKA3-packed exosomes and chemicals including RNAseA, Cytochalasin D, Digoxin or MβCD for 3 days, and processed to gelatin degradation assays (left) and Image-J analysis (right). Ascites from tumor-bearing mice injected with circSKA3-transfected B16 cells showed enhanced gelatin degradation, which could be prevented by RNAseA, Cytochalasin D, Digoxin or MβCD treatment. **, $p<0.01$. Error bars, SD ($n=5$).

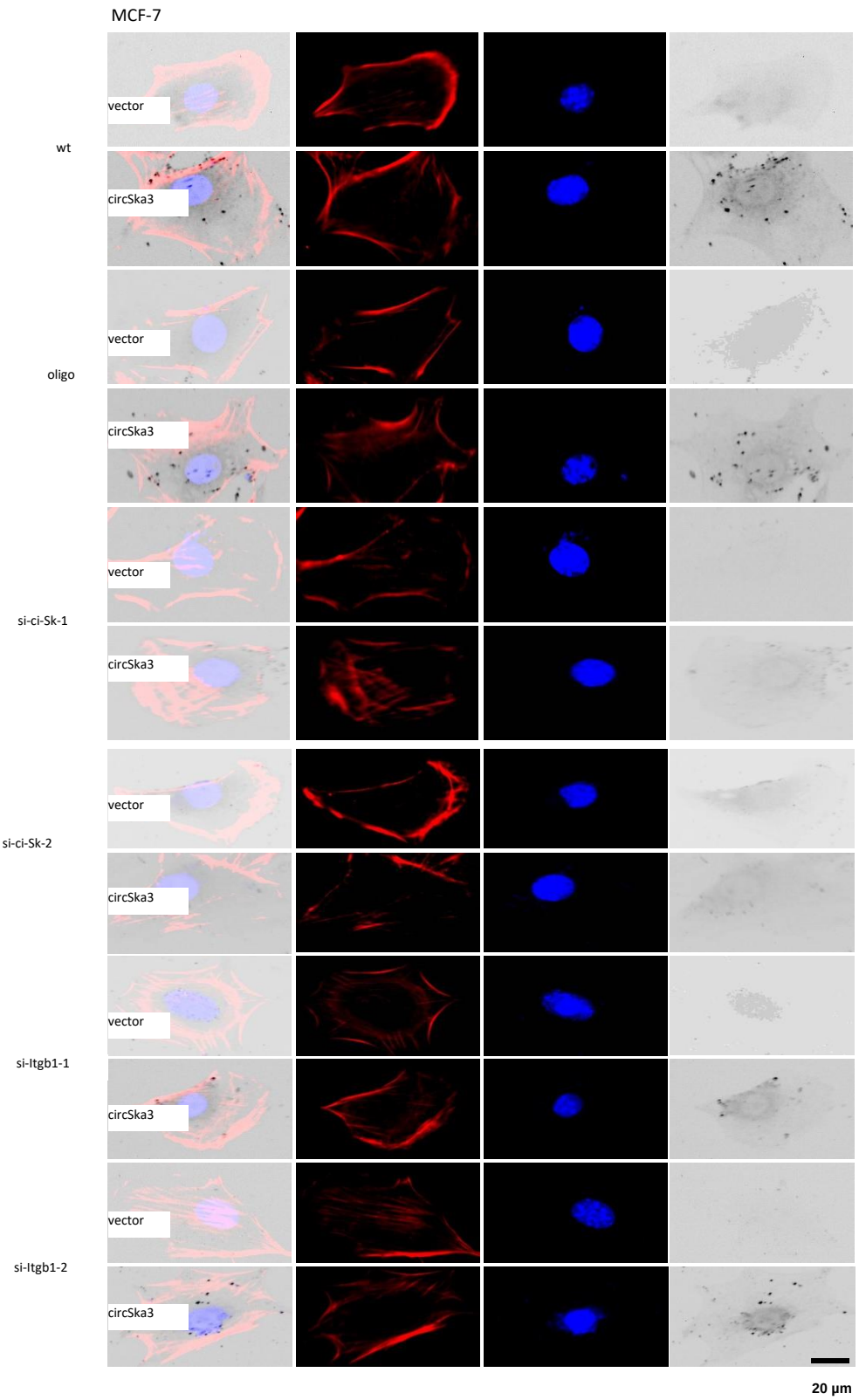

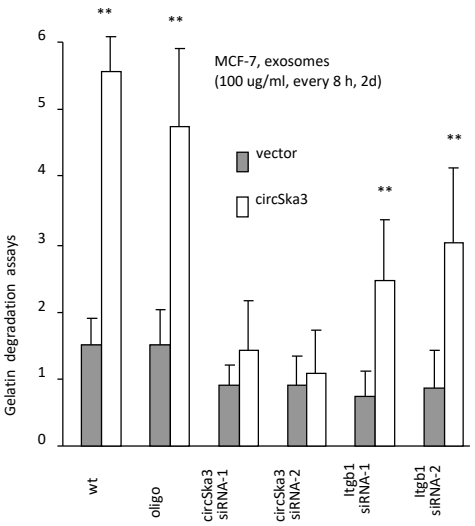

Fig S10. **Dissociation of the complex decreased gelatin invasion.**

(b) MCF-7 cells were transfected with control oligo, circSKA3 siRNA or integrin beta1 siRNA; incubated in vector or circSKA3 packed exosomes for 2 days and proceeded to gelatin degradation assay. Image J analysis showed that delivering circSKA3 packed exosomes enhanced invadopodia formation which could be blocked by silencing circSKA3 but not integrin beta1. ** $p<0.01$, Error bar, SD, (n=6)

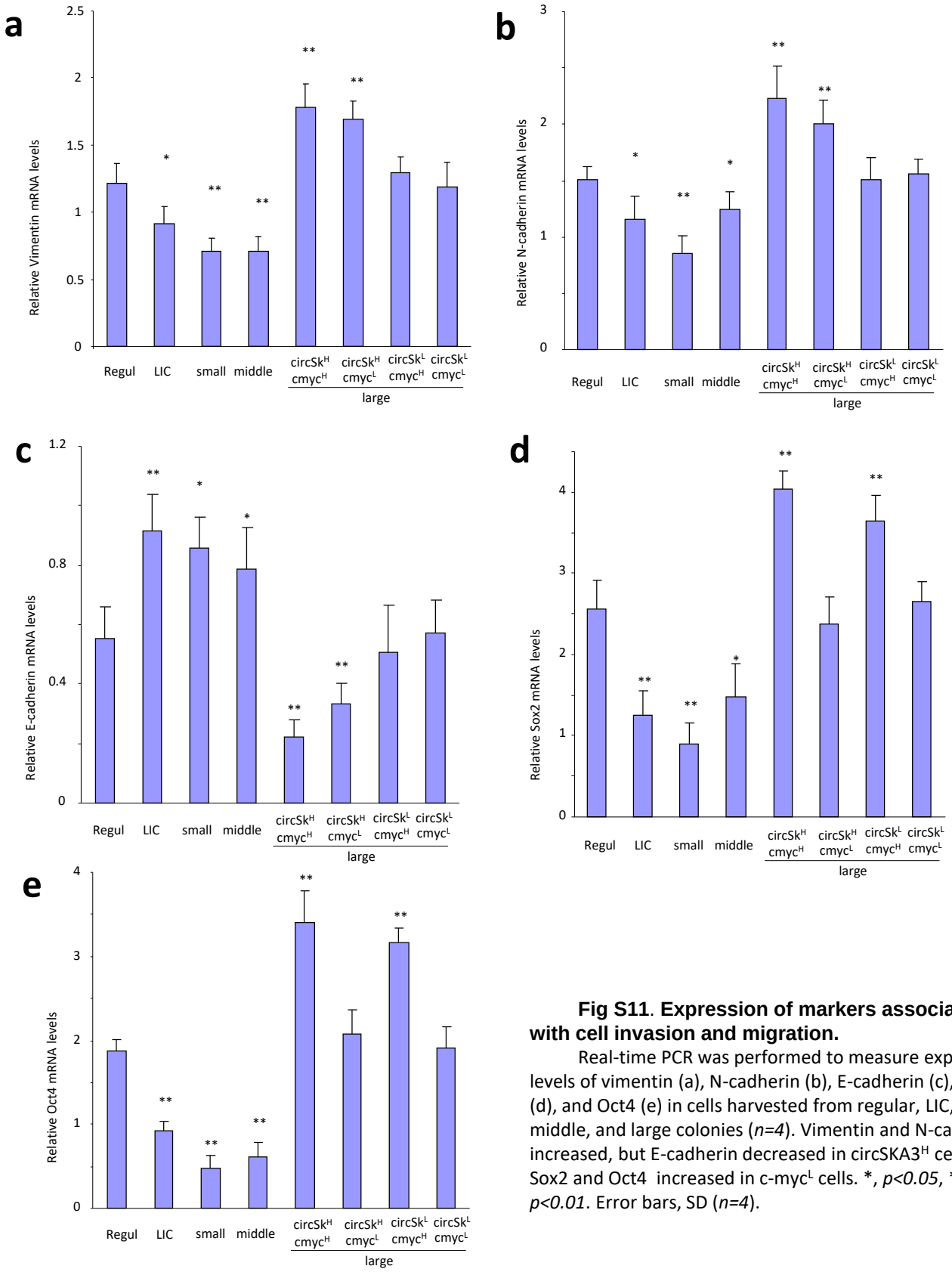

Fig S11. Expression of markers associated with cell invasion and migration.

Real-time PCR was performed to measure expression levels of vimentin (a), N-cadherin (b), E-cadherin (c), Sox2 (d), and Oct4 (e) in cells harvested from regular, LIC, small, middle, and large colonies (*n=4*). Vimentin and N-cadherin increased, but E-cadherin decreased in circSKA3^{H} cells. Sox2 and Oct4 increased in c-myc^{L} cells. *, *p<0.05*, **, *p<0.01*. Error bars, SD (*n=4*).

Supplementary Table S1. Primers used for PCR

29.70.H-coding-Ska3-F	5' gaaggcattgatttcataaaggca
29.12.H-coding.SKA3-R	5’ cag aca gat cat ctttc aca tcag
31.15.hu.Cir.SKA3-R2	5’ cacaattagacaactctgggtcag
31.16.hu.Cir.SKA3-F2	5’ cacaatgggacttaaaaatgcgag
39.41.hu.Vimentin-F.	5’ cttctccgggagccagtccg
39.42.hu.Vimentin-R.	5’ cctgcggtaggaggacgagg
39.43.hu.NCadherin-F.	5’ gcgaatgatcttaggattggg
39.44.hu.NCadherin-R.	5’ gggaattcagcacccgcctc
22-64.Hu-E-cadherin-601F	5’ tcccatcagc tgcccagaaa atga
22-65.Hu-E-cadherin-720R	5’ gtgt ca gc tcctt ggcc ag tg atg
19-71.Hom-Sox2-421F	5’ cgcccgcatg tacaacatga tgg
19-72.Hom-Sox2-660R	5’ tc ggc gccc agg cgc ttg ct gatc
19-73.Hom-c-myc-64F	5’ cgggtag tggaaaacca ggtaagc
19-74.Hom-c-myc-299R	5’ tttccc tct gcc ttc tcct ctccc
19-67.Hom-Oct4-241F	5’ gcgccttcct tccccatggc ggg
19-68.Hom-Oct4-480R	5’ gt ac gcc at cccccc aca taa ctc